

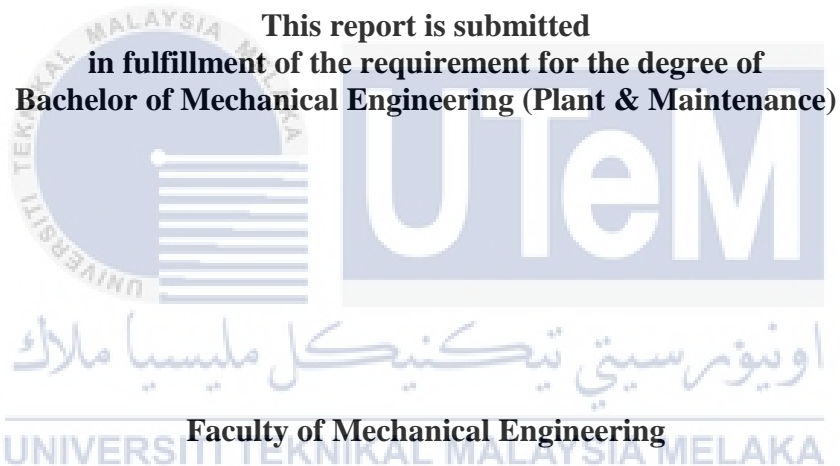
**EFFECT OF WAVE MODULATION MEASURED AT VARIOUS LOCATIONS FOR DAMAGE
DETECTION USING VIBRO ACOUSTIC METHOD**



UNIVERSITI TEKNIKAL MALAYSIA MELAKA

**EFFECT OF WAVE MODULATION MEASURED AT VARIOUS LOCATIONS
FOR DAMAGE DETECTION USING VIBRO-ACOUSTIC METHOD**

NG CHIN SERN



UNIVERSITI TEKNIKAL MALAYSIA MELAKA

2017

DECLARATION

I declare that this project report entitled “Effect Of Wave Modulation Measured At Various Locations For Damage Detection Using Vibro-Acoustic Method” is the result of my own work except as cited in the references

Signature	:
Name	:
Date	:



اونيورسيتي تيكنيكل مليسيا ملاك

UNIVERSITI TEKNIKAL MALAYSIA MELAKA

APPROVAL

I hereby declare that I have read this project report and in my opinion this report is sufficient in terms of scope and quality for the award of the degree of Bachelor of Mechanical Engineering (Plant & Maintenance).

	Signature	:
	Name of Supervisor	:
	Date	:



اونيورسيتي تيكنيكل مليسيا ملاك

UNIVERSITI TEKNIKAL MALAYSIA MELAKA

DEDICATION

To my beloved mother and father



ABSTRACT

Structural Health Monitoring has greatly developed in recent years where more advanced method was studied and applied practically in our daily lives. Among the most commonly applied in the method is the nonlinear acoustic effect excite simultaneously with low frequency. This application has been researched to determine the reliability to detect fatigue crack in specimen. In general, every material in this world is restricted to certain period of life span. There are 3 stages of fatigue failure development from the initiation of micro crack up to the fracture of the material. Crack formation is then classified into 3 modes where the mode is depends on the manner force applied on the plate. The fatigue crack propagation does not increase proportional with the number of load cycles. An aluminum plate is prepared into the required specification in order to proceed with the vibro-acoustic test. The natural frequency is determined through modal analysis and then the mode shape was confirmed using the VL scanning software. Then the first 3 mode shape frequency was excited for the vibro-acoustic analysis where the location of measurement was distributed into 25 points above the crack line. Based the modulation intensity (R-value) at each points, an analysis was done on the graph of R-value against measurement point distance from crack. Lastly, a contour plot was produced to ease the understanding on modulation intensity distribution on the measurement points for all 3 modes.

اونیورسیتی تکنیکل ملیسیا ملاک

UNIVERSITI TEKNIKAL MALAYSIA MELAKA

ABSTRAK

Pemantauan kesihatan struktur telah kian maju dimana semakin banyak kaedah canggih dikaji dan dipraktikkan dalam kehidupan seharian. Antara kaedah-kaedah yang lazim digunakan adalah kesan akustik tidak linear yang dirangsang serentak dengan frekuensi rendah. Penggunaan kaedah telah dikaji keandalannya untuk mengesan retak lesu dalam spesimen. Secara amnya, setiap bahan dalam dunia ini mempunyai jangka hayat yang tertentu. Terdapat 3 peringkat retak lesu yang bermula dengan retak mikro sehingga fraktur. Formasi retak ini dibahagi kepada 3 mod bergantung pada cara daya tekanan yang diaplikasi pada plat. Perkembangan retak lesu ini tidak meningkat secara linear dengan bilangan kitaran daya tekanan. Sekeping plat aluminium disediakan mengikut spesifikasi tertentu dan dilanjutkan dengan kajian vibro akustik. Frekuensi resonan ditentukan melalui analisis modal dan bentuk mod menggunakan perisai pengimbasan VL. 3 frekuensi mod pertama dirangsang untuk analisis vibro akustik di mana lokasi pengukuran dibahagi kepada 25 titik di atas garis retakan. Analisis dijalankan melalui bandingan intensiti modulasi (R -value) di 25 titik dan graf diplot R -value berbanding jarak lokasi pengukuran dari garis retakan. Akhir sekali, plot kontur diplot untuk memudahkan perbandingan dan pemahaman intensiti modulasi pada lokasi pengukuran untuk ketiga-tiga frekuensi mod.

اوتنورسي تيكنيكل مليسيا ملاك

UNIVERSITI TEKNIKAL MALAYSIA MELAKA

ACKNOWLEDGEMENTS

First of all, I would like to express my deep gratitude and appreciation to my supervisor Dr.Ruztamreen bin Jenal from Faculty of Mechanical Engineering Universiti Teknikal Malaysia Melaka for his guidance, support and encouragement throughout the whole project. His suggestion and idea has helped me in conducting the project effectively in achieving my project objective.

My appreciation also extends to my panels Dr. Roszaidi bin Ramlan and Mdm Norasra binti Rahman for their advice and evaluation on improving my report writing. Other than that, I would like to thanks all technical staff that helped me during preparing specimen till conducting the experiment for the project. They are Mr.Azhar and Mr.Wan Saharizal who is the lab assistant engineer at Cubic and Fasa B respectively.

Also I would not forget my supervisor master student, Mr.Tino who has always gives a helping hand when I face problem during conducting the experiment.

Above ground, I would deliver my special thanks to all my parents, siblings and peers for their moral support and encouragement in completing this project. Finally, I offer my regards and blessing to those who has gave me help and support during the project.

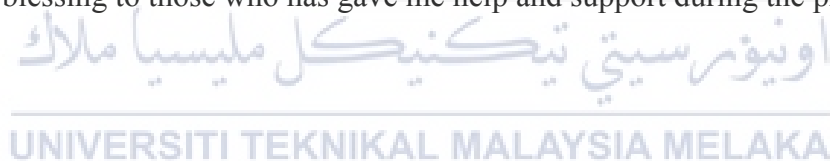


TABLE OF CONTENTS

DECLARATION	ii
APPROVAL	iii
DEDICATION	iv
ABSTRACT	v
ABSTRAK	vi
ACKNOWLEDGEMENTS	vii
TABLE OF CONTENTS	viii
LIST OF TABLES	x
LIST OF FIGURES	xi
LIST OF ABBREVIATIONS	xiii
CHAPTER 1 INTRODUCTION	1
1.1 Background	1
1.2 Problem Statement	4
1.3 Objectives	4
1.4 Scope of Project	5
CHAPTER 2 LITERATURE REVIEW	6
2.1 Damage in structure	6
2.2 Fatigue crack	7
2.3 Methods to detect fatigue crack	9
2.3.1 Nonlinear Acoustics	9
2.3.2 Finite Element Method (FEM)	11
2.4 Vibro-acoustic method	13

2.5	Nonlinear Vibro-Acoustic Effects	16
2.5.1	Harmonic Generation	16
2.5.2	Amplitude Modulation and Sidebands Generation	16
CHAPTER 3 METHODOLOGY		18
3.1	Research Methodology	18
3.2	Material preparation	20
3.3	Experimental Setup	24
3.4	Modal Analysis	26
3.5	Vibro-Acoustic test	30
CHAPTER 4 RESULTS AND DISCUSSION		35
4.1	Material specification	35
4.2	Modal Analysis	37
4.3	Vibro Acoustic Test	39
4.4	Discussion	45
CHAPTER 5 CONCLUSION & RECOMMENDATION		46
REFERENCES		47

LIST OF TABLES

TABLE	TITLE	PAGE
Table 3-1:	Parameter of the mechanical properties of aluminum plate obtained from Tensile Test.....	22
Table 3-2:	Input parameter for modal analysis.....	27
Table 3-3:	Matlab coding for conversion to frequency response function with explanation.....	27
Table 3-4:	Matlab coding for conversion to FFT with explanation	31
Table 3-5:	Categories measurement points to respective zone.....	33
Table 4-1:	Material properties of the aluminum plate.....	35
Table 4-2:	Vibration mode with respective frequency	38
Table 4-3:	Vibration mode with respective mode shape	38
Table 4-4:	Average R value based on the 1 st sideband.....	39
Table 4-5:	Average R value based on the 2 nd sideband.....	40
Table 4-6:	Average R value based on the 1 st + 2 nd sideband.....	40
Table 4-7:	Overall result of highest and lowest R-value from the 3 type of sideband analysis	43

LIST OF FIGURES

FIGURE	TITLE	PAGE
Figure 1-1:	Approaches of Infrared Thermography	4
Figure 2-1	Modes of degradation	6
Figure 2-2:	Stages of fatigue failure development	7
Figure 2-3:	Three basic modes of fatigue crack in plate	8
Figure 2-4:	Effect of crack length and stress level on crack propagation rate	9
Figure 2-5:	Schematic figure of cross modulation between pump wave and probe wave.....	11
Figure 2-6:	Sideband amplitude ratio over the fundamental frequency amplitude	12
Figure 2-7:	Standard analytical formula.....	12
Figure 2-8:	The ratio of first sideband amplitude over fundamental frequency amplitude, R value, against the ultrasound frequency results (a) receptance analysis and (b) FEM and (c) the average R value against crack size with various damping factors.....	13
Figure 2-9:	Setup of Vibro-Acoustic Method using impact hammer.....	14
Figure 2-10:	Setup of Vibro-Acoustic Method using shaker	14
Figure 2-11:	Experimental arrangement using PZT transducer and stack actuator on an aluminum plate [33].....	15
Figure 3-1:	Flowchart of the project.....	19
Figure 3-2:	EDM hole drilling machine	20
Figure 3-3:	Dimension of hole drilling location.....	21
Figure 3-4:	EDM wire cutting machine.....	21
Figure 3-5:	Result after EDM wire cut with (a) the enlarged result.....	22
Figure 3-6:	Result displayed in system controller monitor	23
Figure 3-7:	Fatigue crack on the aluminum plate with (a) enlarged crack picture.....	24

Figure 3-8: Experiment setup for the modal analysis and vibro-acoustic test.....	25
Figure 3-9: Location of equipment placement on the aluminium plate	26
Figure 3-10: Flowchart on setting up VL software	29
Figure 3-11: Distribution of measurement points on the aluminum plate.....	30
Figure 3-12: Amplitude modulation with notation of sidebands for calculation of R-value.....	32
Figure 3-13: Distribution of measurement points separated by zone based on distance from crack.....	33
Figure 4-1: Fatigue crack length on the aluminum plate.....	36
Figure 4-2: FFT result from Matlab (a) original scale (b) magnified scale.....	37
Figure 4-3: Average R-value against distance from crack for 1 st sideband analysis.....	41
Figure 4-4: Average R-value against distance from crack for 2 nd sideband analysis	42
Figure 4-5: Average R-value against distance from crack for 1 st + 2 nd sideband analysis	43
Figure 4-6: Distribution of R-value on the aluminum plate by exciting (a) 1 st , (b) 2 nd , and (c) 3 rd vibration modes.	44

اوتورسیتی تکنیکل ملیسیا ملاک

UNIVERSITI TEKNIKAL MALAYSIA MELAKA

LIST OF ABBREVIATIONS

SHM	Structure Health Monitoring
NDT	Non-Destructive Test
NDE	Non-Destructive Evaluation
PZT	Piezoelectric Transducer



CHAPTER 1

INTRODUCTION

1.1 Background

In the 21st century, diagnosis and early evaluation on the degree of structure damage has become more crucial. The most general approach of this task is Structural Health Monitoring (SHM) in order to sustain the safety, reliability and performance of the structure. This application is extensively used in various type of structure such as aircraft, bridges and buildings. SHM is a non-destructive scientific process of identifying four characteristics real-time or near real-time related to fitness of an engineered system as it operates using a built-in sensory and reasoner system. The four characteristics are [1]:

- a. Operational and environmental loads acting on a component
- b. Mechanical damage caused by the load
- c. Growth of damage as the component operates
- d. Future performance of the component as damage accumulates.

In such, there are several advanced non-destructive test/evaluation (NDT/NDE) widely used in various engineering fields to fulfil the definition. In 2004, there are several NDT techniques that have been summarized [2] [3].

Dye penetration where a liquid or penetrant such as chalk is applied on a cleaned and low roughness material surface. Then the penetrant will infiltrates the surface's flaw which will reveal the place where penetrant crept in. This characteristic makes it possible to detect a micro crack which is only 0.00005 mm wide.

Magnetic particle method uses the principle that a flaw in magnetic material produces distortion in an induced magnetic field. This is a simple and most sensitive method in NDT to apply even along complex geometries. Due to the fact that this method can be applied on a very large surface of component at once, it has a very high potential to be fully automated and production line integrated [4].

Eddy-current testing is a method which based on physics phenomenon of electromagnetic induction. A probe that consists of a wire coil and generated oscillating magnetic field is brought close to a conductive material such as metal piece. Then a circular flow of electrons or better known as eddy current will begin to move across the metal and will generate its own magnetic field which interacts with the coil. Any changes in the thickness or defect along the surface cracking will affect the amplitude and pattern of the eddy current and the magnetic field [5].

Ultrasound method transmits an ultrasonic wave into a test material and any defects in the material will reflect a pulse wave and the reflected waves are measured. Then the waves will be digitized leads to a change of the echo shape in comparison with an analogue display. This enable a better visualisation on defect which is only hit by one ultrasonic shot [6]. However, it is very tough to distinguish between cracks and other types of defect where it has a limited application toward specific specimen geometry.

Along with the advancement of technology, improvement in NDT methods allows mankind to use better sensor, material technology, new analysis tools and software for better damage detection or structural health monitoring. Among these advanced methods is guided wave inspection, infrared thermography, acoustic and etc..

Guided wave has been applied in solids such as seismology, inspection, material characterisation, delay lines and etc. [7]. Among the main class of these waves is Lamb waves and Rayleigh wave which is dispersive plate wave and surface wave respectively.

These waves can propagate in any solid structure which has boundaries as it is essential element for guided waves. Guided waves are a group of waves at which various modes is in superposition. The phenomenon is due to the stress and strain condition of the boundaries [8].

Infrared thermography is another approach of advanced NDT for damage detection which is fast, non-contact and able to cover a wide area of inspection in compared with the conventional NDE techniques. Basically any object above the absolute zero temperature will emit infrared radiation which makes this method so useful. There are two general approaches which is passive, where the feature of interest is naturally contrast temperature than the background. The active approach is where an energy source is required to produce thermal contrast between the feature of interest and the background. Generally, most of the cases will apply the active approach as the feature of interest temperature is normally in equilibrium with the surrounding. Then in the active approach it is divided into external, energy is transfer to the surface and then propagated through the material until a flaw is encountered. It is commonly performed with optical devices such as photographic flashed or halogen lamps. Other than that is internal active approach, where energy is injected into the material to stimulate exclusively the defects. The energy is normally excites by using mechanical oscillations like sonic or ultrasonic transducer. A summary of infrared thermography approaches is as in Figure 1-1 [9].

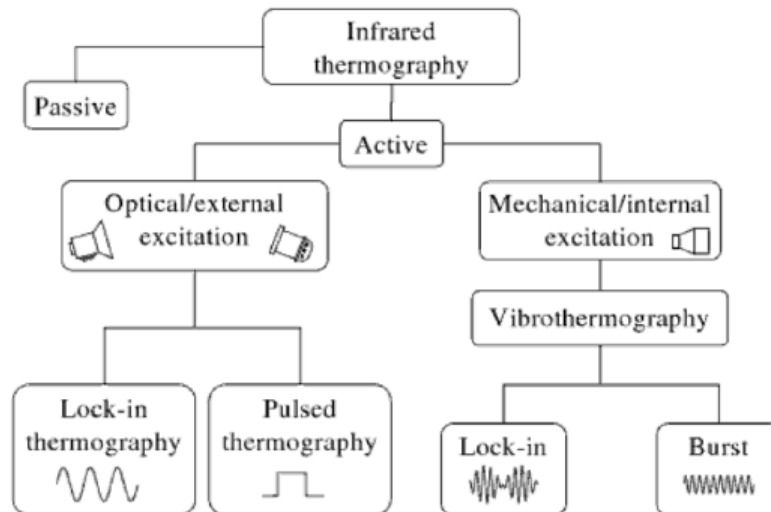


Figure 1-1: Approaches of Infrared Thermography

1.2 Problem Statement

Vibro-acoustic is one of the methods to determine the fatigue crack which uses the propagation of high frequency acoustic waves in solid structure with low frequency excitation. Therefore, several parameters should be considered in order to obtain an effective result. Among the parameters are:

- a) Low frequency excitation location and frequency
- b) High frequency excitation location and frequency
- c) Location of measurement point

1.3 Objectives

There are several parameters which will affect the wave modulation of the experiment. However, this study would focus on the effect of the measurement point location towards the wave modulation effect from low and high frequencies excite to detect the crack.

1.4 Scope of Project

The scopes of this project are:

1. Sample preparation which consists of 4 procedures in order to begin the experiment which is:
 - Cutting a piece of aluminum plate to the required dimension.
 - Drilling hole to allow line cutting
 - Line cutting in order to initiate fatigue crack
 - Create fatigue crack
2. Modal analysis to determine the aluminum plate vibration modes
 - Sweep frequency excitation to determine the natural frequency
 - VL scanning software to determine the relevant mode shape.
 - Obtain the first 3 modes shape.
3. Non-linear vibro-acoustic test to determine effect of various measurement points towards the modulation intensity in fatigue crack detection.
 - Distribute 25 measurement points above the crack which is 30 mm apart each point.
 - Analyse R-value based on 1st sideband analysis, 2nd sideband analysis and 1st + 2nd sideband analysis.

Analyse contour plot of individual R-value on the aluminum plate.

CHAPTER 2

LITERATURE REVIEW

2.1 Damage in structure

Structure is defined as the system for transferring of loads from one place to another [10]. Damage can be defined as the deviation in structure from its original geometric or material properties that caused by unacceptable stress, displacement or vibration in the structure [11]. There are two most common mode of degradation and failure is due to the localised phenomena such as crack propagation at reduced cross sections. One of the mode would have lesser noticeable degradation in the initial cycles and the once the degradation occurs it would happen with a very fast rate. This will show the degradation process covering only a very small portion of the material life-span. Then another mode the degradation threshold is very small where the degradation occurs at a slower rate with the number of cycles. Based on the flow, it would cover up a larger portion of degradation in the life-span of the material. The summarised modes of degradation are as in Figure 2-1 [12].

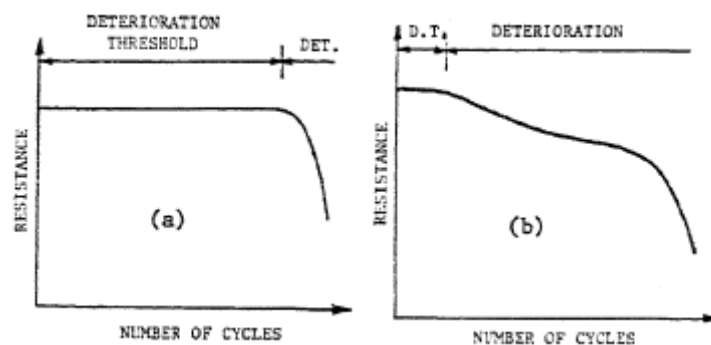


Figure 2-1 Modes of degradation

Among the damage in structure, the most commonly discussed is the damage initiation in fatigue behaviour of a material. The damage due to fatigue is hard to be identify because the nucleation damage in pristine can be large part of the total fatigue life. Not only that, for every different material the crack dimension might vary from a microscopic scales up to few millimetres depending on the structure and application [13].

2.2 Fatigue crack

Fatigue failure is defined as the failures due to stresses repeating for a larger number of times. Basically it consists of three stages for the fatigue failure development starting with stage 1 where the initiation of micro cracks due to cyclic plastic deformation. However, at this stage of process it is not visible to naked eyes where people overlooked. Then it followed with stage 2 where propagation of micro crack to macro cracks forming parallel plate like fracture surfaces separated by longitudinal ridges. This is the stage where users begin to realise the development before it fracture. Lastly is stage 3, the fracture stage where the material could not support the loads any longer. All the process is picturised as in Figure 2-2 [14].

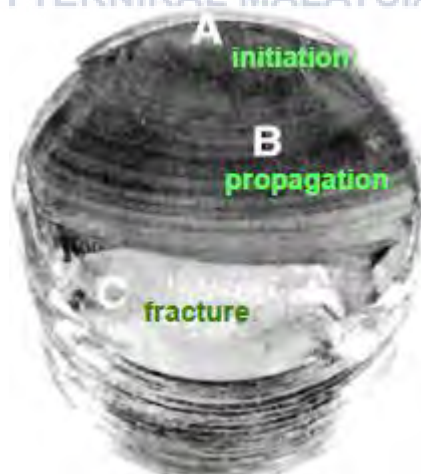


Figure 2-2: Stages of fatigue failure development

Crack formation on the plate can be distinguish in several manner based on the force applied on the plate. Mode I is the opening mode where the body of material is loaded by tensile forces such that it is pulled apart in the y-axis. Mode II, the sliding mode where material body is loaded by shear forces that is parallel to the crack surface in the x-axis. Mode III is tearing mode where the body is loaded with shear forces parallel to the crack front the crack surface. However, in some cases all the three modes might happen in a mixed situation or can be called as superposition situation. Combination of the 3 modes can be illustrated as in Figure 2-3 [15].

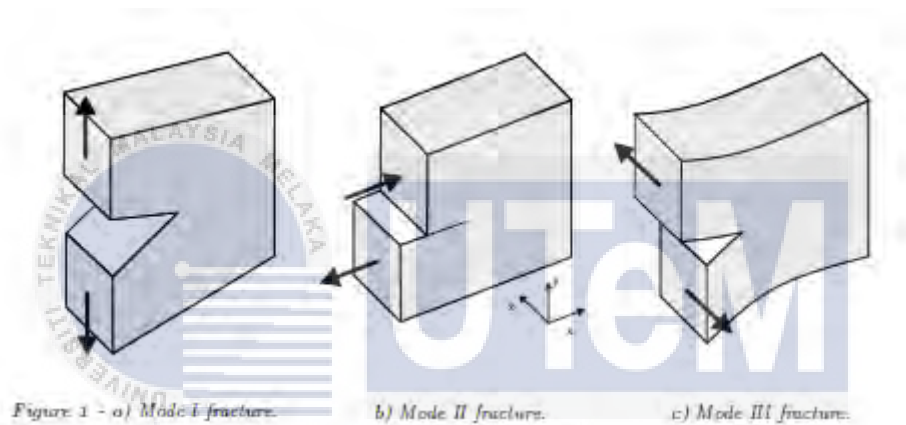


Figure 2-3: Three basic modes of fatigue crack in plate

Once the fatigue crack is present in the material, the crack propagation is noticeable that in such crack length increases with number of loading cycles. It could also be seen that the crack growth rate would increase with the increasing crack length. Then the growth rate of the crack increases with the developing stress level. The crack process becomes longer with a rapid rate where the crack does not increase linearly with the number of loading cycles. However, lots of the loading cycles concerned in the complete life of the component are consumed during the early levels of the crack extension. The summary of the elemental parameters of the fatigue crack growth is as in Figure 2-4 [16].

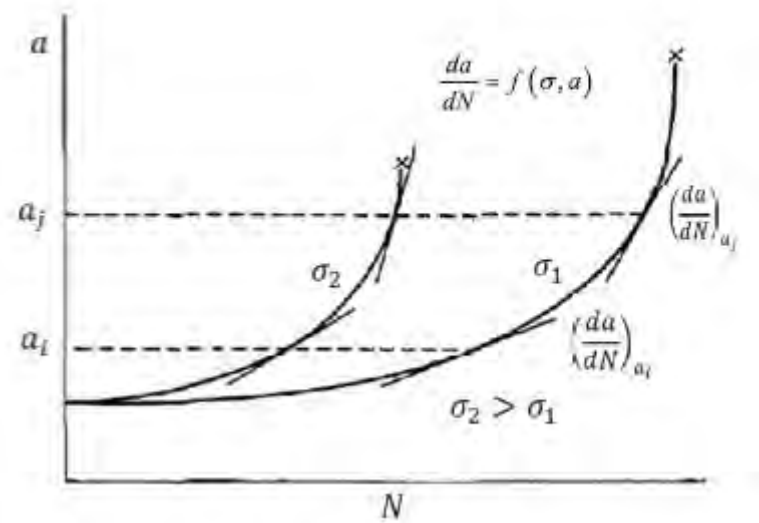


Figure 2-4: Effect of crack length and stress level on crack propagation rate

2.3 Methods to detect fatigue crack

2.3.1 Nonlinear Acoustics

In up to date years, nonlinear effect from acoustic wave has been widely studied in order to detect damage [17, 18]. This is because the method allowed early detection on micro damage and it is easier to detect in compared with the traditional linear measurement [19, 20]. There are several common nonlinear effects that strongly dependant on the wave propagating medium such as generation of side bands, amplitude dissipation, generation of harmonics and resonant waves shifting. Nonlinear effects for instance amplitude modulation is commonly known as interaction of the wave with micro-inhomogeneous medium [21]. Therefore it has been a common finding in most of the studies on nonlinear effect that correlated with defects such as discontinuities present in the medium.

Back in the 1970s, nonlinear acoustics has been thoroughly studies by Rudenko, Zaitsev and many others. There are lots of reports on the nonlinear effect of elastic wave propagation in metals, polymers and soils being used to detect failures. In 1979, Morris et al. used second harmonic generation in order to supervise the evolution of fatigue cracks in

aluminum alloy [22]. Then in 1994, Korotkov et al uses sound modulation excitation by vibration to detect defects in steel [23]; Nagy in 1998 uses nonlinear ultrasonic characterisation to detect fatigue crack in plastics, metals, composites and adhesives [24]. Then in late 2000, Van Den Abeele et al. demonstrated the propagation of harmonics and sidebands as a result of damaged properties in Plexiglass and sandstones [25].

Among the most paramount finding is by Donskoy and Sutin (1999) [26] using the modulation of ultrasound by low frequency vibration to detect defects like cracks, debonding and delamination in steel pipe. Then in the same year, Zheng et al. uses nonlinear acoustic imaging to interpret the degree of material disturbance cause by the asymmetry of lattice structure and disorder in crystals [27].

In general, nonlinear acoustic wave modulation is the interaction between acoustic waves and the low frequency vibration. This has been the parameter practically studied in order to measure the degree of damage in a material. Then in year 2000, Van Den Abeele et al. present a new technique called Nonlinear Elastic Wave Spectroscopy (NEWS) where this technique excite two frequencies at the same time to a specimen in order to detect damage [28]. The detection is based on the inspection on the harmonics and sidebands of the frequencies excites on the specimen [28]. Advancement of technologies enable the used of low-profile piezoceramic actuator and lead zirconate titanate (PZT) transducer to introduce synchronously low-frequencies excitation and high-frequencies ultrasonic waves accordingly to the test specimen [17, 29]. Degree of sidebands around the high-frequency peak were analysed in order to identify micro crack. Novel nonlinear-modulation method was proposed for crack detection using cross modulation effect generated from a gradually increasing amplitude-modulated firm excitation and a probe signal. The schematic figure is shown as in Figure 2-5 [30].

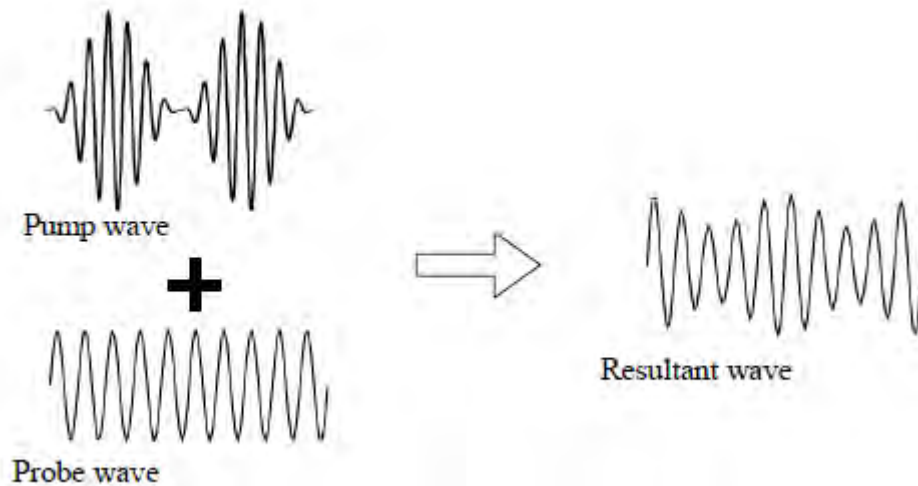


Figure 2-5: Schematic figure of cross modulation between pump wave and probe wave

Based on the effects of nonlinear acoustics several experimental works and analytical modelling works have been conducted in order to detect defects such as cracks.

2.3.2 Finite Element Method (FEM)

This is a numerical technique in obtaining a predictive solution to boundary value dispute by using partial differential equation. The rapid advancement in computing and software technology has allowed this method to be efficient and dependable in solving problem.

In order to justify the receptance analysis method, FEM was used to model a beam as close as possible on actual beam with a cracked geometry. The crack was modelled with no boundary limit nodes along the crack line. Then natural frequency and mode shape value of the beam model were figure out and the results were substituted into equation in Figure 2-6 and Figure 2-7 in order to obtain the R value.

$$R = \frac{2}{\pi} \frac{|H_o(f_0) - H_c(f_0)|}{|H_o(f_0) + H_c(f_0)|} = \frac{2}{\pi} \frac{B_1}{B_0}$$

where H_o and H_c are transfer function values when the crack is fully open and closed

$$B_0 = \frac{H_o + H_c}{2} \text{ is mean value of the modulation signal}$$

$$B_1 = \frac{H_o - H_c}{2} \text{ is the peak-to-peak variation around the modulation}$$

Figure 2-6: Sideband amplitude ratio over the fundamental frequency amplitude

$$H_y(\omega) = \sum_n \frac{u_i^n u_j^n}{\omega_n^2 + i\omega_n \omega / Q_n - \omega^2}$$

where $H_y(\omega)$ denotes transfer function value at frequency ω between points i and j .

$u_{i,j}^n$ is mode shape value at location i/j for mode n

ω_n is natural frequency at mode n

Q_n is damping factor at mode n

Figure 2-7: Standard analytical formula

Based on the analysed result, it has shown the dependence of R value on the fundamental frequency. Not only that, the sensitivity effect of the nonlinear acoustics method in detection of damage might also affected by the damping factor. The results is shown as in Figure 2-8 which include results based on receptance analysis, FEM and also the average R value against crack size with various damping factors [33].

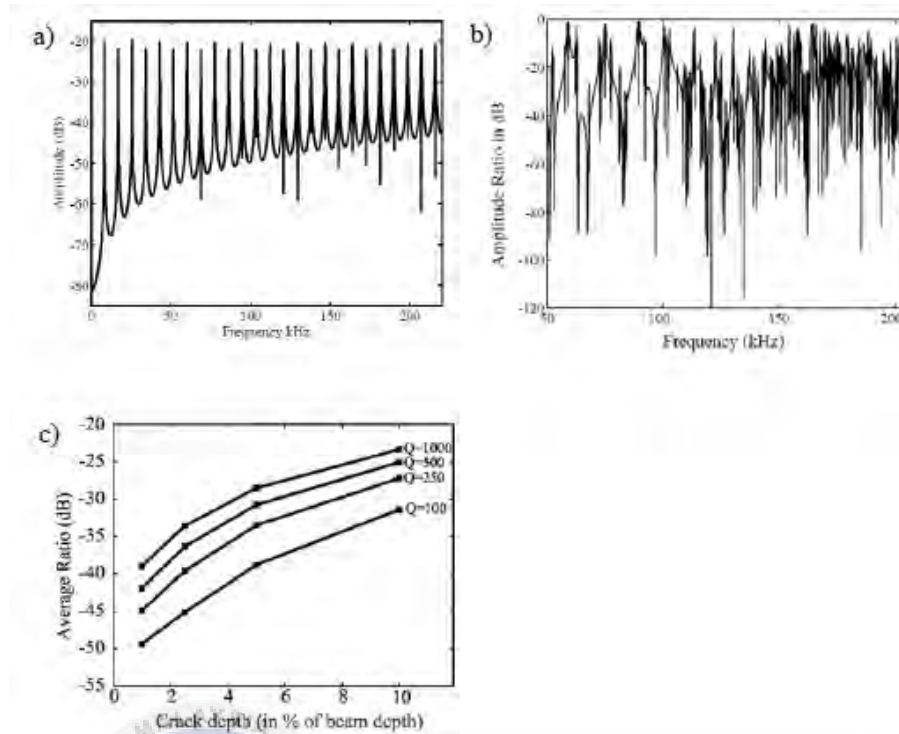


Figure 2-8: The ratio of first sideband amplitude over fundamental frequency amplitude, R value, against the ultrasound frequency results (a) receptance analysis and (b) FEM and (c) the average R value against crack size with various damping factors.

2.4 Vibro-acoustic method

Practically there are several method applied the amplitude modulation of high-frequency ultrasound by low-frequency vibration excitation. Among of it is the Vibro-Acoustic Method [34, 35] or Nonlinear Wave Modulation Spectroscopy (NWMS) [36, 37, 38]. Basically there are 2 types of Vibro-Acoustic Method setup. The general setup is by hanging the specimen on elastic string in order to reduce boundary effect during the assessment. The first type uses an impact hammer where the most dominant mode is excite into the specimen as in Figure 2-9.

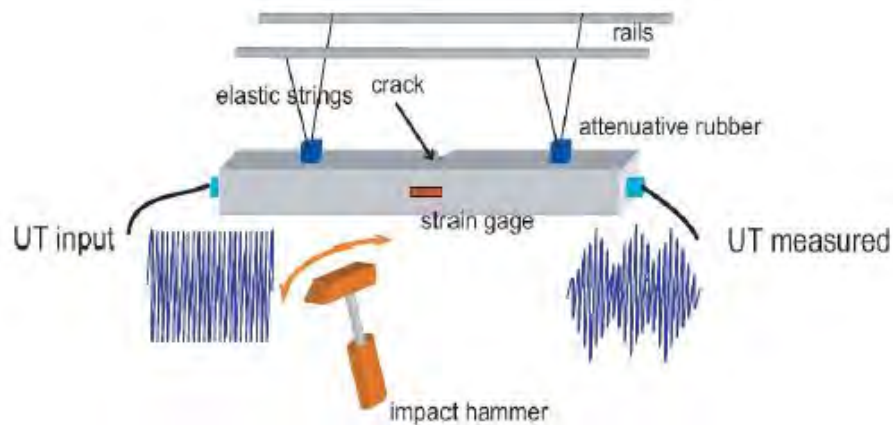


Figure 2-9: Setup of Vibro-Acoustic Method using impact hammer

Evaluation on the effect sensitivity against the defect sizes is based on the first sideband effects. Then the connection between the sideband effect and experiment parameters such as ultrasonic frequency, loads and low-frequency vibration was also been analysed. Researcher has then determined with a relevant combination of low amplitude low-frequency vibration and precise frequency range of ultrasonic signals, it could be a NDT tool for damage detection.

Lots of researchers have then replace the impact hammer with a controlled shaker in order to vibrate the specimen as shown in Figure 2-10.

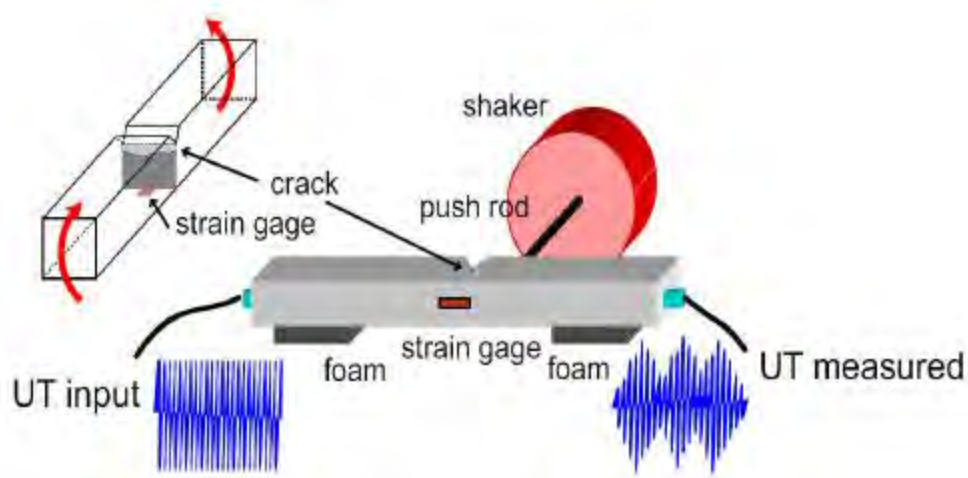


Figure 2-10: Setup of Vibro-Acoustic Method using shaker

This new method is more stable in exciting the low-frequency vibration in compared with the preceding one. Yet the interaction between the shaker attached to the specimen might causes the degree of noise increases and additional nonlinear acoustic effects in frequency spectrum.

Due to the advancement in technologies, Parson et al. [16] used a piezo-ceramic stack actuator to excite the specimen as in Figure 2-11. The specimen is hanged using an elastic string and a significantly reduced size of stack actuator in order to compromise the method for diagnosing defects using nonlinear acoustic effects. By using this method, the nonlinear effects and noise from the mechanical shaker and solid supports can be avoided. The experiment conducted was compared with the method using mechanical shaker for excitation. The con of the method is that the maximum excitation degree of the piezo-ceramic stack actuator is relatively lower than the mechanical shaker. However the result from this method has shown a better signature in term of sidebands effect against defects [33].

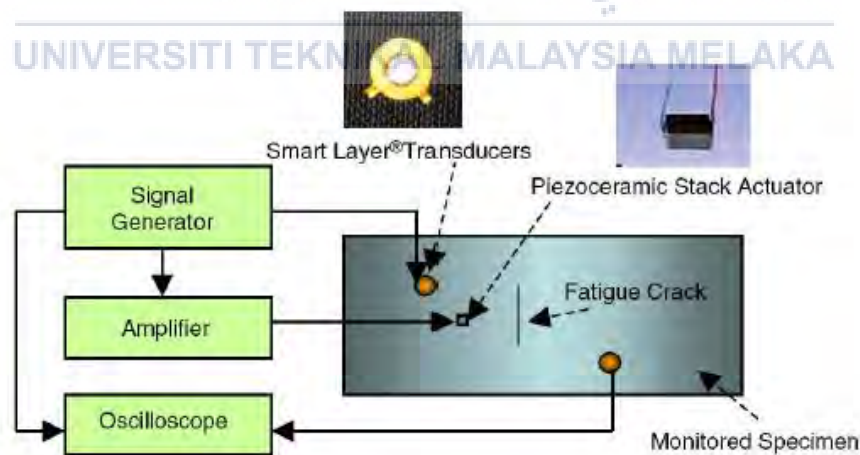


Figure 2-11: Experimental arrangement using PZT transducer and stack actuator on an aluminum plate [33].

2.5 Nonlinear Vibro-Acoustic Effects

There are several effects which was studies by researchers to validate the used of vibro-acoustic method in detecting crack.

2.5.1 Harmonic Generation

Non-linear acoustics has been proven to be an effective method in order to detect material defect [39], [40]. Then harmonic imaging was widely used in medical diagnostics where the harmonic displayed from wave propagation in the medium would be recorded [41], [42]. Crack closure and the harmonic generation were achieved by progressively applying a compressive load with present of high voltage excitation [43]. There are also successful studies that were done identifying the effect of dislocation motion towards harmonic generation [44], [45]. Among the aluminum related study was completed and justify by Buck et.al where he uses surface wave to determine the present of fatigue stress in aluminum [46]. A study on the effect of longitudinal vibration beam on the higher harmonic generation resulting in the crack delocalisation. The analysis shows amplitude of the harmonic generated increases with the proximity of crack [47]. There is also documentation on the harmonic amplitude response against the fundamental wave amplitude [48].

2.5.2 Amplitude Modulation and Sidebands Generation

Amplitude modulation happens when there are two frequencies linked and one of it is varying the amplitude. However, both the frequencies are not closed together. The higher frequency is known as the carrier frequency while the lower frequency is the modulated frequency. Then sidebands generated would has interval between sidebands is equal to the low frequency signal. There are several researchers who have applied the

sidebands from nonlinear acoustic method to detect damage in Non-Destructive Evaluation (NDE) such as Sutin, Staszewski and others.

There are studies was done to validate the capability of modulation effect to detect damage and this method was used in damage detection in structure components [26], [49], [50], [51]. Other than that, studies was also done on several other material such as rocks, concretes, composites, metals and bonding material [52], [30], [53], [54], [55], [56].

The sensitivity of amplitude modulation effects on the material nonlinearities has been widely studied and justified. There is a modified method which uses an averaging ratio of first sideband amplitude over the ultrasonic amplitude in determining the modulation intensity or the R value [29], [33], [55]. The calculation of the R value is written as

$$R = \frac{A_1 + A_2}{A_0}$$

where the A_0 is the ultrasonic amplitude, $A_1 + A_2$ is the summation of first sideband amplitude on the right and left of the ultrasonic spectrum.

The averaging of the modulation intensity is written as

$$M_{\pm n} = \sum_{m=1}^M \frac{A_{m \pm n}}{A_m A_n}$$

Where m is the integer indicating the number of ultrasonic wave, n is the number of vibration modes, $A_{m \pm n}$ is the averaged sideband amplitude, A_m vibration amplitude and A_n the ultrasonic wave amplitude.

CHAPTER 3

METHODOLOGY

3.1 Research Methodology

This chapter will explain on the process in order to complete the project. A proper planning and commissioning is essential to ensure a proper and great outcome of the project. In every project, the most basic step is to have a good planning and task time frame for the whole project. The project is divided into 3 phases which is the material preparation, modal analysis and vibro-acoustic method. First of all, information required is divided into sub parts and each of it is studied by comparison on the existing methods that are published in paper. The required specification and dimension of material is sketched and the dimension of hole and slot on the material is fixed in the drawing. The flow of the methodology is included in Figure 3-1.

UNIVERSITI TEKNIKAL MALAYSIA MELAKA

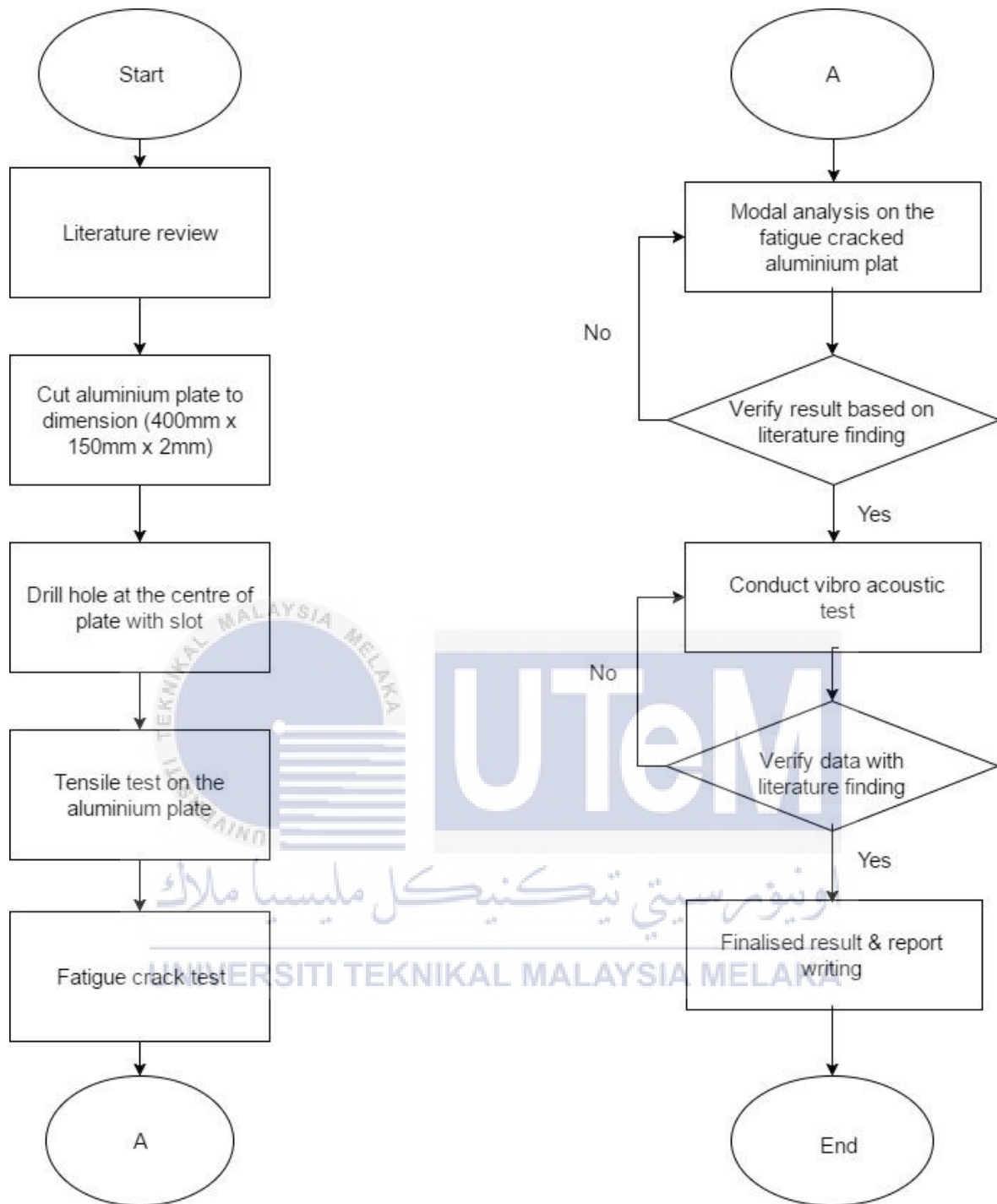


Figure 3-1: Flowchart of the project

3.2 Material preparation

The initial task is to have a simple and compact drawing to give a better picture when cutting and drilling the specimen to required specification. Project begins with cutting the aluminum plate into the required dimension 150mm x 400mm x 2mm. This process uses a shearing machine in order to increase the accuracy of dimension cut. After the cutting process was done, the dimension of the plate was re-measured using a measuring tape to ensure the aluminum plate is up to the required dimension. Then the centre of the plate was determine and marked to drill a hole of diameter 1mm. As the diameter is very precise, an electrical discharged machine (EDM) hole drilling machine was used as in Figure 3-2.

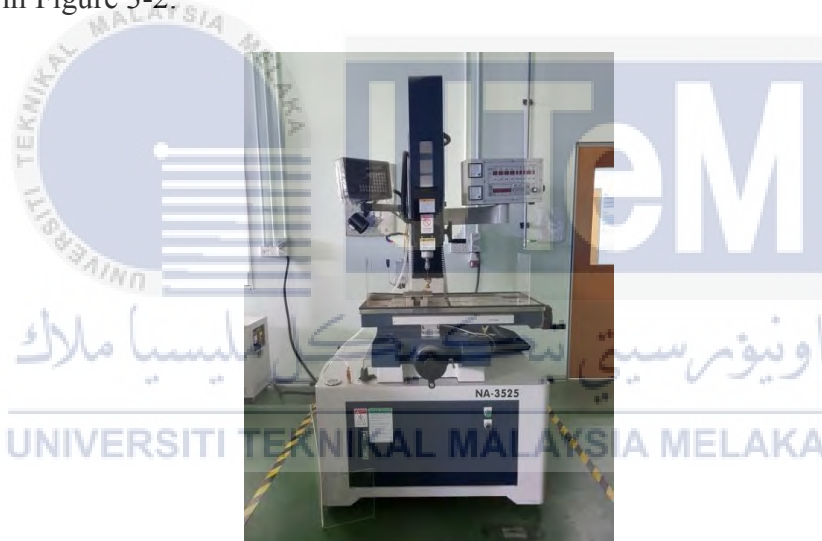


Figure 3-2: EDM hole drilling machine

However there is a tolerance of maximum ± 0.5 mm which might happen due to the inaccuracy of the machine. The location of the hole is at 200 mm x 75mm of the plate as in Figure 3-3.

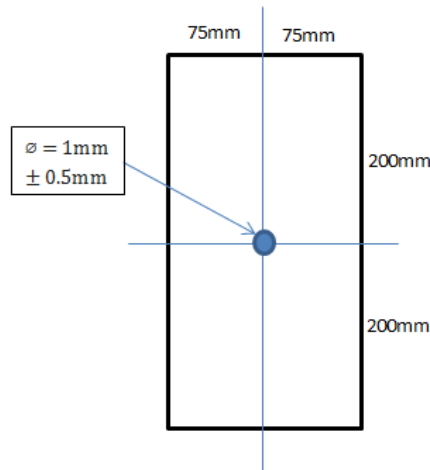


Figure 3-3: Dimension of hole drilling location

Next was followed by cutting a slot which is 1mm off from the circumference of the hole drilled by using electrical discharge wire cut machine as in Figure 3-4.



Figure 3-4: EDM wire cutting machine

The size of the wire used for the cutting is 0.2mm as the required slot size should be smaller in compared to the hole drilled. This step is used to ease the process of creating a fatigue crack. Result after the EDM wire cut is shown in Figure 3-5.

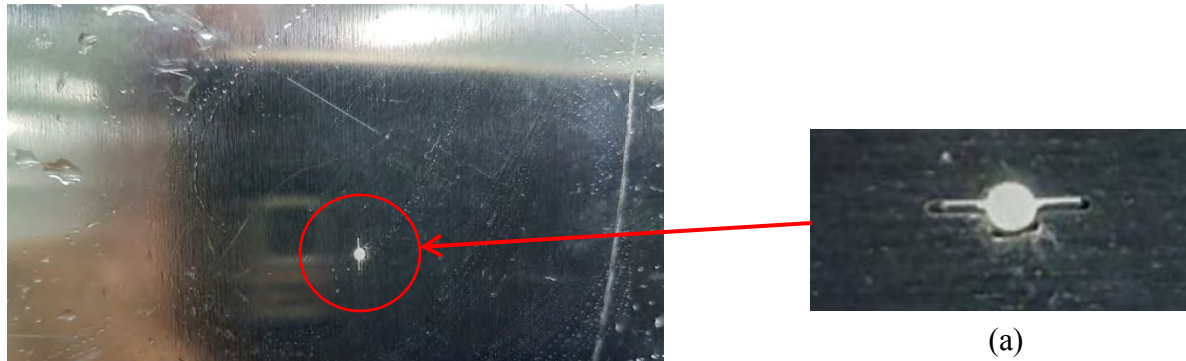


Figure 3-5: Result after EDM wire cut with (a) the enlarged result

Then an aluminum plate of the same dimension was used to conduct tensile test using the universal testing machine. This is to obtain the load against extension graph with the tensile strength of the material as in Table 3-1

Table 3-1: Parameter of the mechanical properties of aluminum plate obtained from Tensile Test.

	Maximum load for yield (kN)	Tensile stress at maximum load for yield (MPa)	Maximum load (kN)	Tensile stress at maximum load (MPa)
1	> 35.62	> 118.73	35.62	118.73

Based on the result obtained, the maximum load, minimum load, mean load, amplitude was determined to proceed with initiating the fatigue crack.

Maximum load = 75% of yield load

$$= 0.75 \times 35.62$$

$$= 26.715 \text{ kN}$$

Minimum load = 0.1 of maximum load

$$= 0.1 \times 26.715$$

$$= 2.67 \text{ kN}$$

$$\text{Mean load} = \frac{\text{Maximum load} + \text{Minimum load}}{2}$$

$$= \frac{26.715 + 2.67}{2}$$

$$= 14.6925 \text{ kN}$$

$$\text{Amplitude} = \frac{\text{Maximum load} - \text{Minimum load}}{2}$$

$$= \frac{26.715 - 2.67}{2}$$

$$= 12.03 \text{ kN}$$

The following step is to create the fatigue crack on the aluminum plate by applying cyclic loading using the universal testing. Then set the machine type of loading into cyclic and sinusoidal. Next is entering the parameters of maximum load, minimum load, mean load, amplitude based on the calculated data.

Fatigue crack of 10mm is able to be obtained after 89205 cyclic load amplitude and range of loading between 2.67 kN to 26.7 kN with the frequency of 10 Hz. The data is displayed on the system as shown in Figure 3-6.



Figure 3-6: Result displayed in system controller monitor

A minimum length of 10mm from the centre of slot fatigue crack was created. The fatigue crack present in the aluminum plate is as in Figure 3-7.

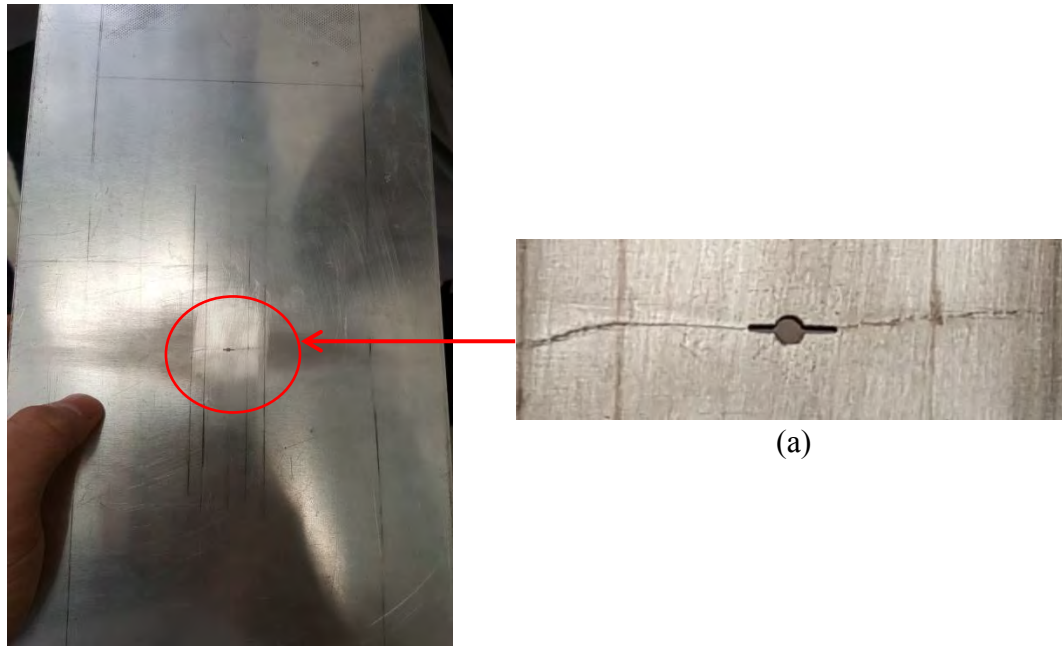


Figure 3-7: Fatigue crack on the aluminum plate with (a) enlarged crack picture

3.3 Experimental Setup

This project uses the experimental modal analysis in order to determine the natural frequencies of the aluminum plate. Low frequency is excited using the shaker while high frequency uses a piezoceramic transducer. Then the measurement of vibration uses the digital SWIR scanning laser Doppler vibrometer which is more accurately target on specific location. The setup of apparatus and equipment is as in Figure 3-8.

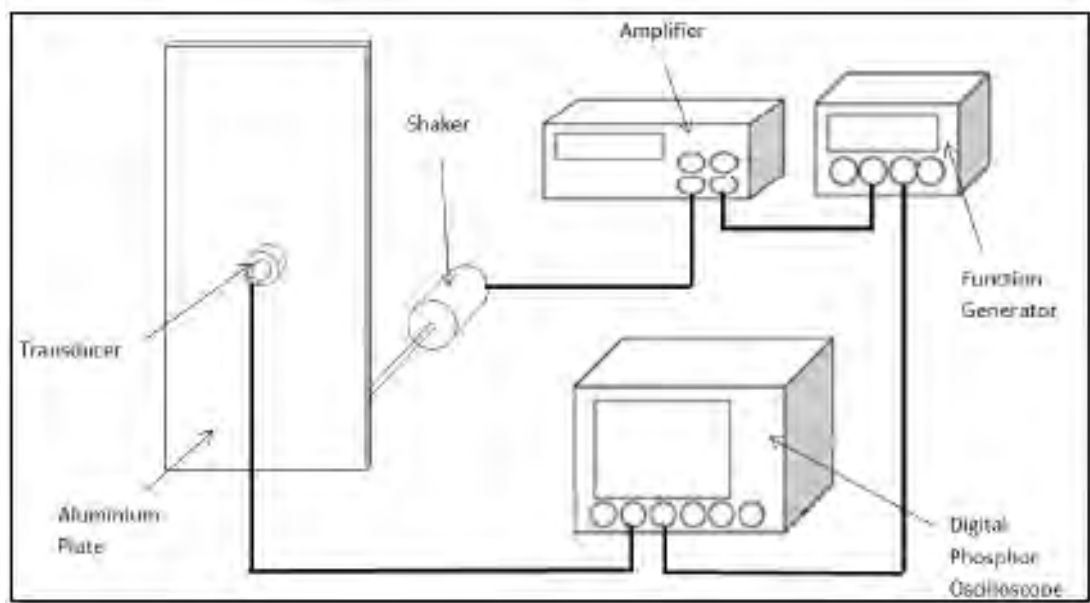


Figure 3-8: Experiment setup for the modal analysis and vibro-acoustic test

The aluminum plate was suspended freely using a string. A shaker was adhesively glued on the back of the plate located 20mm from the edge. Then a piezo ceramic transducer was placed 60mm below the cracked line. The measurement point of the laser is 60mm above the cracked line and the distance of SWIR scanning laser Doppler vibrometer from the plate is 1314mm. Location and distance of the equipment placement is shown as in Figure 3-9.

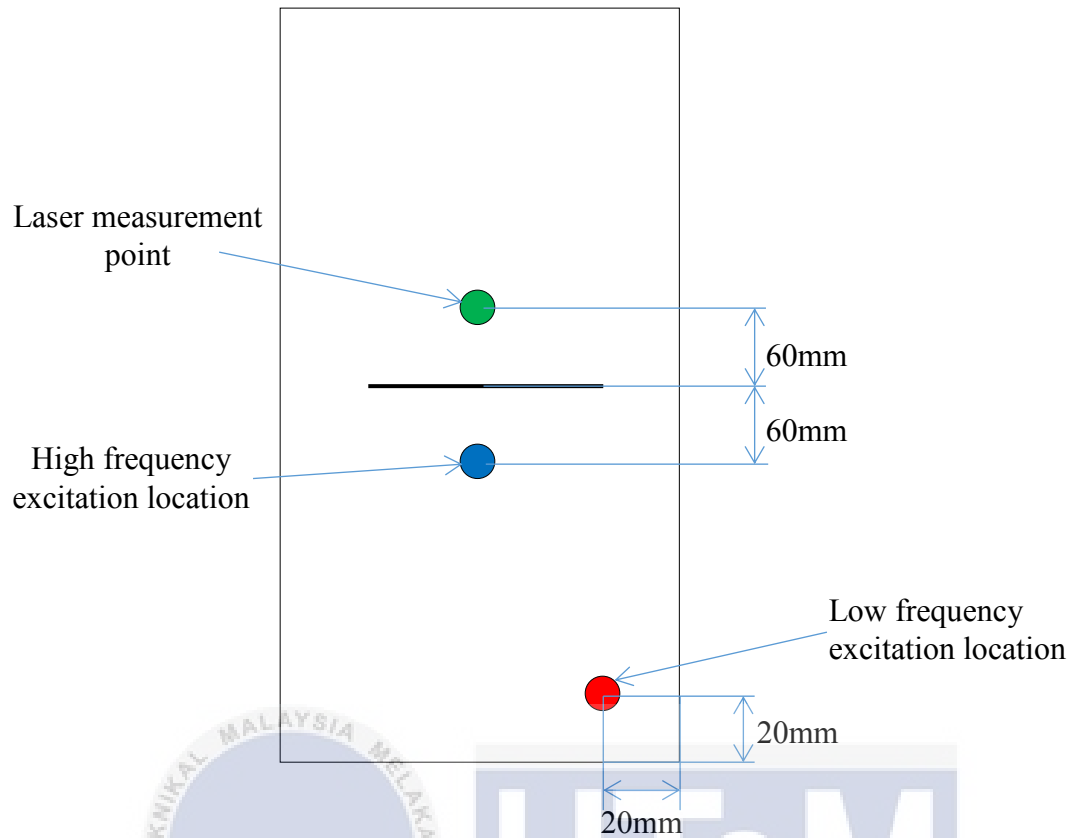


Figure 3-9: Location of equipment placement on the aluminium plate

3.4 Modal Analysis

In order to determine the mode shape, sweep frequency excitation needed to be done on the aluminum plate. This was done using the Tektronix AFG 3022C dual channel arbitrary function generator with appropriate parameters. The input parameter for the modal analysis is as in Table 3-2.

Table 3-2: Input parameter for modal analysis

Items	Parameter
Sweep frequency	1 – 2000 Hertz
Sweep time	2s
Amplitude	5.0 Vpp
Sampling size	10kS/s
Number of sample	100k samples

On the measurement using the laser, no filter applied when conducting the sweep frequencies excitation. Then the result of excitation will then be analyse and converted into frequency response function using Matlab software. The coding used to determine the frequencies mode is shown in Table 3-3.

Table 3-3: Matlab coding for conversion to frequency response function with explanation

Coding	Function
<pre>x1=xlsread('in.xlsx'); x2=xlsread('in1.xlsx'); x3=xlsread('in2.xlsx'); x4=xlsread('in3.xlsx'); x5=xlsread('in4.xlsx');</pre>	- Importing the input frequency data.
<pre>y1=xlsread('out.xlsx'); y2=xlsread('out1.xlsx'); y3=xlsread('out2.xlsx'); y4=xlsread('out3.xlsx'); y5=xlsread('out4.xlsx');</pre>	- Importing the output frequency data.
<pre>t = xlsread('time out.xlsx');</pre>	- Import sampling time and time derivative.

<code>dt = mean (diff(t));</code>	
<code>Fs = 1 / dt;</code>	- Obtain the sampling frequency.
<code>[Txy1,f] = tfestimate(x1,y1,[],[],[],Fs);</code> <code>Txy1dB = 20*log10(abs(Txy1));</code> <code>[Txy2,f] = tfestimate(x2,y2,[],[],[],Fs);</code> <code>Txy2dB = 20*log10(abs(Txy2));</code> <code>[Txy3,f] = tfestimate(x3,y3,[],[],[],Fs);</code> <code>Txy3dB = 20*log10(abs(Txy3));</code> <code>[Txy4,f] = tfestimate(x4,y4,[],[],[],Fs);</code> <code>Txy4dB = 20*log10(abs(Txy4));</code> <code>[Txy5,f] = tfestimate(x5,y5,[],[],[],Fs);</code> <code>Txy5dB = 20*log10(abs(Txy5));</code>	- Determine transfer function estimate, time-invariant transfer function [TF,f]. - Convert the magnitude of data to decibel (dB).
<code>TxydBavg = (Txy1dB + Txy2dB + Txy3dB + Txy4dB + Txy5dB) / 5;</code>	- Determine the average of TxydB.
<code>plot (f,TxydBavg);</code>	- Plot a graph of f against TxydB.
<code>xlim ([0 2000])</code> <code>ylim ([-100 40])</code>	- Limit the plot of x-axis from 0 to 2000. - Limit the plot of y-axis from -100 to 40.
<code>xlabel ('Frequency(Hz)')</code> <code>ylabel ('Amplitude (dB)')</code>	- Labelling the graph.

Based on the result of FFT determined from Matlab, the obtained first three frequency mode in the result was then confirmed the mode shape using VL scanning software. The values determined from the mode frequencies is the low frequency which is excite using the shaker. High frequency was excited at 60 kHz at the same location as shown in Figure 3-9. This allowed the motion of the aluminum plate under the specific frequency to be observed. The process flow chart is as in Figure 3-10.

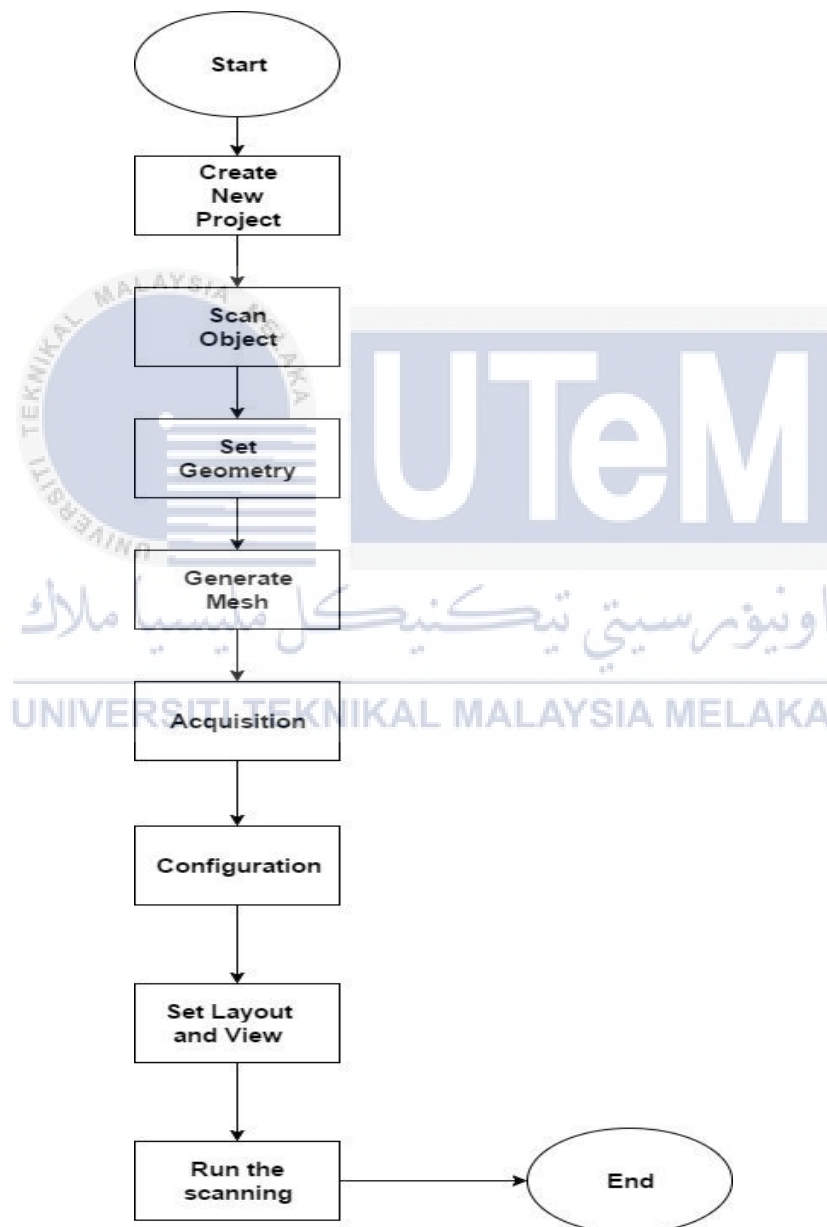


Figure 3-10: Flowchart on setting up VL software

3.5 Vibro-Acoustic test

Overall setup remained the same except for the SWIR scanning laser Doppler vibrometer measurement location. The measurement points were distributed into 25 points located above the cracked line where the distance between each point vertically and horizontally is 30 mm apart. The distance from the cracked line to the high frequency excitation transducer and nearest measurement point is 60mm. For all the points it was numbered to ease the calculation and analysis task. The illustration of the plate designation is as in Figure 3-11.

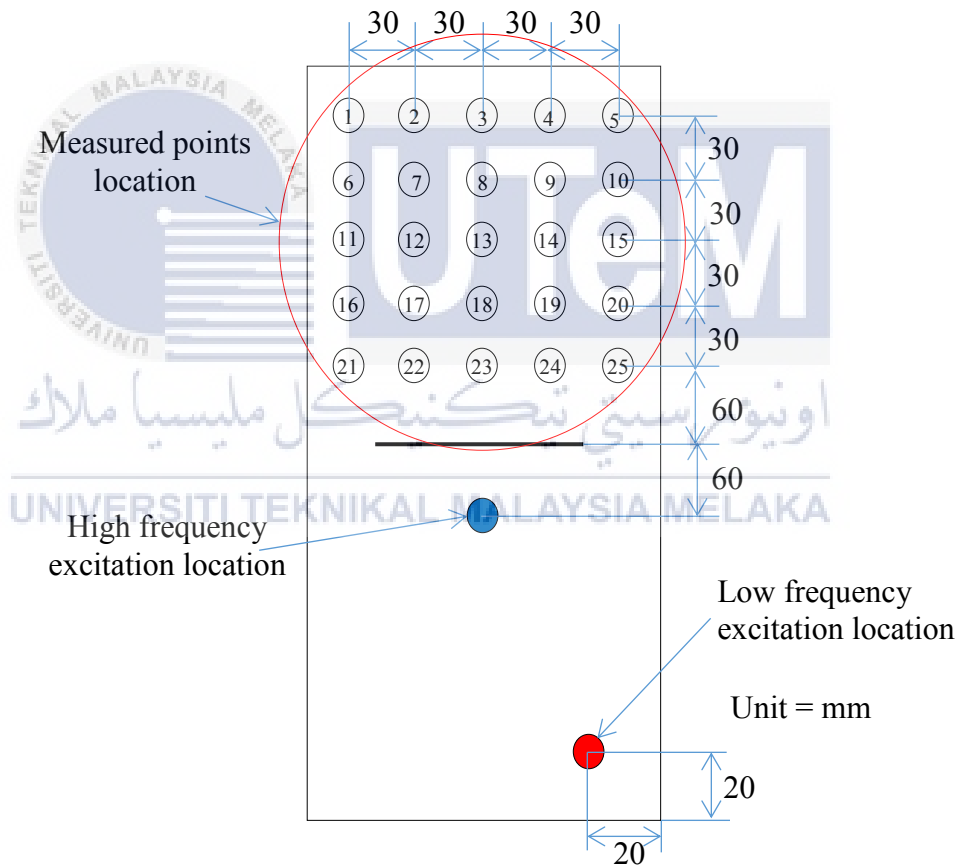


Figure 3-11: Distribution of measurement points on the aluminum plate

The vibro acoustic experimental analysis was conducted by exciting the frequency value determined from modal analysis. It was conducted by using the first three mode

shape frequency excite using the shaker. The excitation of high frequency was kept constant at 60 kHz throughout the experiment. Then for each of the low frequency excite, the measurement was taken at 25 points above the cracked line. The output data was obtained from the Tektronix DPO4032 oscilloscope where it is in the form of time domain. Then the output data was converted to Fast Fourier Transform using Matlab software. The coding for the conversion is as shown in Table 3-4.

Table 3-4: Matlab coding for conversion to FFT with explanation

Coding	Function
<code>data = csvread('1.csv') ;</code>	- Import data
<code>time = data(:,1);</code> <code>signal = data(:,2);</code>	- Read data based on array
<code>Ts = mean(diff(time));</code> <code>Fs = 1/Ts;</code>	- Obtain the sampling frequency
<code>L=length(signal);</code>	- Set length of vector
<code>NFFT = 2^nextpow2(L);</code>	- Determine the new input length
<code>freq = -Fs/2+Fs/NFFT:Fs/NFFT:Fs/2;</code>	- Obtain the frequency for plotting
<code>Y = fft(signal,NFFT)/L;</code> <code>Ycent = fftshift(Y);</code> <code>ya = sgolayfilt(Ycent,10,27);</code>	- Shift the zero frequency component to center of spectrum - Filtering to smoothen the graph
<code>figure(1),</code> <code>plot(freq,abs(ya));</code>	- Plot graph of frequency against FFT signal
<code>title('Single-Sided Amplitude Spectrum of y(t)');</code> <code>xlabel('Frequency (Hz)');</code> <code>ylabel(' Y(f) ');</code>	- Name title and axis
<code>xlim([0 100000])</code> <code>ylim([0 0.00035])</code>	- Setting limit of x axis from 0 to 100000 - Setting limit of y axis from 0 to 0.00035

From the conversion, the FFT graph would be used to determine the modulation intensity or R-value. The formula of R-value used is written as

$$R = \frac{A_1 + A_2}{A_0}$$

$$R = \frac{A_3 + A_4}{A_0}$$

where A_0 is the ultrasonic amplitude, $A_1 + A_2$ is the summation of first sideband amplitude on the right and left of the ultrasonic spectrum, $A_3 + A_4$ is the summation of second sideband amplitude on the right and left of the ultrasonic spectrum.

The peak of A_0, A_1, A_2, A_3, A_4 is as shown in Figure 3-12.

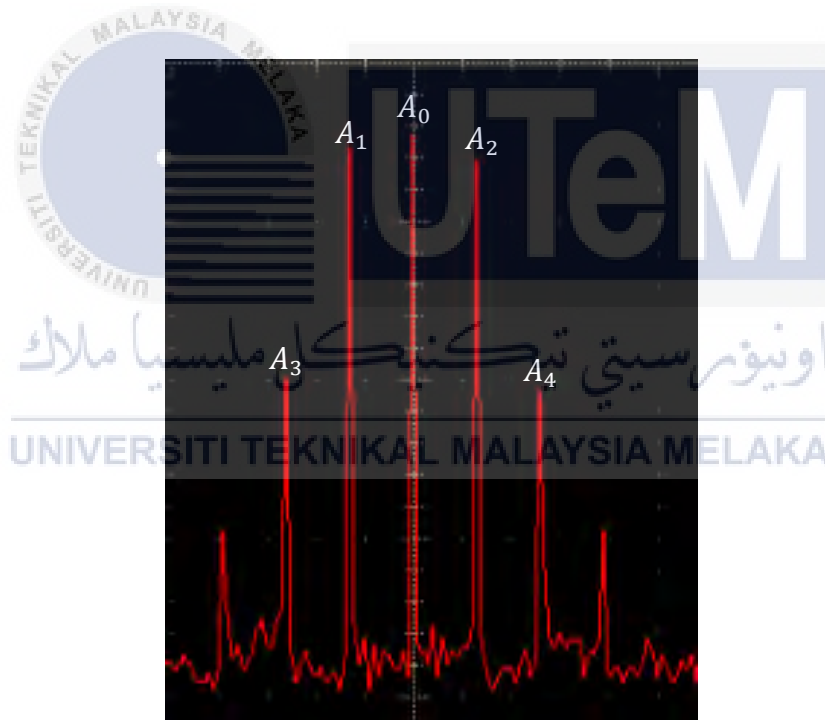


Figure 3-12: Amplitude modulation with notation of sidebands for calculation of R-value

The R-value of the 3 frequencies mode at 25 measurement points was determined. The measurement points were divided into 5 zones at which each zone has its specific distance from the crack. This is to ease the averaging of R value by distance to analyse. The illustration of zones is shown in Figure 3-13.

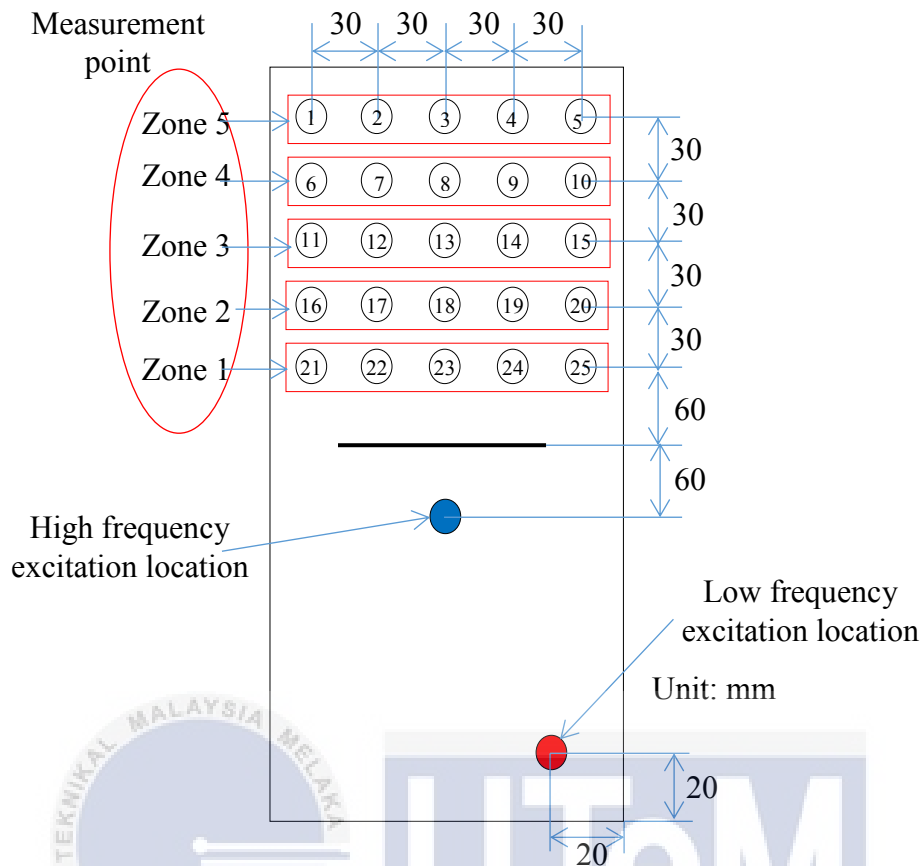


Figure 3-13: Distribution of measurement points separated by zone based on distance from crack.

As shown in figure above, the zone was tabulated as in Table 3-5.

Table 3-5: Categories measurement points to respective zone

Zone	1	2	3	4	5
Distance from crack (mm)	60	90	120	150	180
Measurement point	21, 22, 23, 24, 25	16, 17, 18, 19, 20	11, 12, 13, 14, 15	6, 7, 8, 9, 10	1, 2, 3, 4, 5

For each zone, the average R-value was obtained to plot graph of modulation intensity against distance from crack. Other than that, contour plot was done individually for each vibration mode in order to provide a better illustration of R value distribution on the aluminum plate.



CHAPTER 4

RESULTS AND DISCUSSION

4.1 Material specification

The material used is a 150 mm × 400 mm × 2 mm aluminum plate. Then the material properties are determined as aluminum AL2024 which has a high strength and good fatigue resistance. It is normally used in aircraft structure as a fuselage structure, member of the wing tension and also structural areas. The properties are as in Table 4-1.

Table 4-1: Material properties of the aluminum plate

Property name		Details
Material	Name	Aluminum AL-2024
	Density	2780 kg/m ³
	Young's Modulus	72400 MPa
	Poisson's ratio	0.33

As the distribution of load on the aluminum plate is not proportional, there is a slight different in term o crack length propagation. The current fatigue crack is as in Figure 4-1.

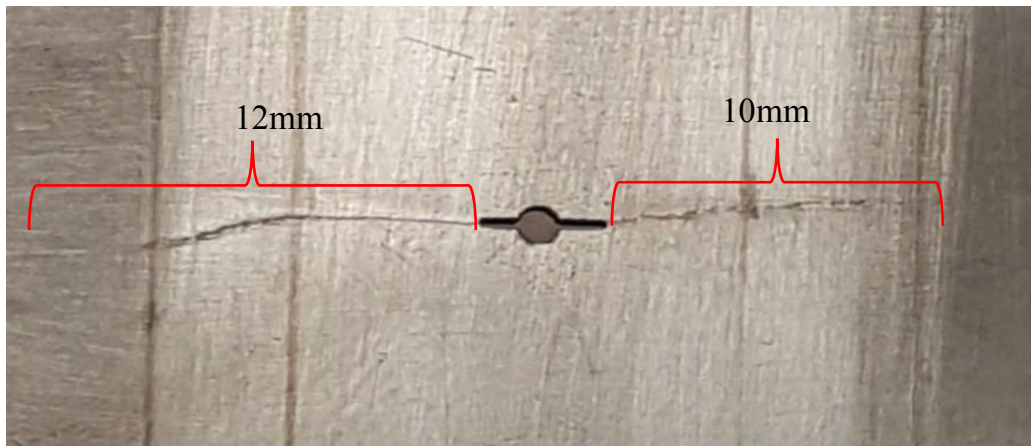


Figure 4-1: Fatigue crack length on the aluminum plate.



4.2 Modal Analysis

From the conversion done using Matlab, the result was obtained as show in Figure 4.2.

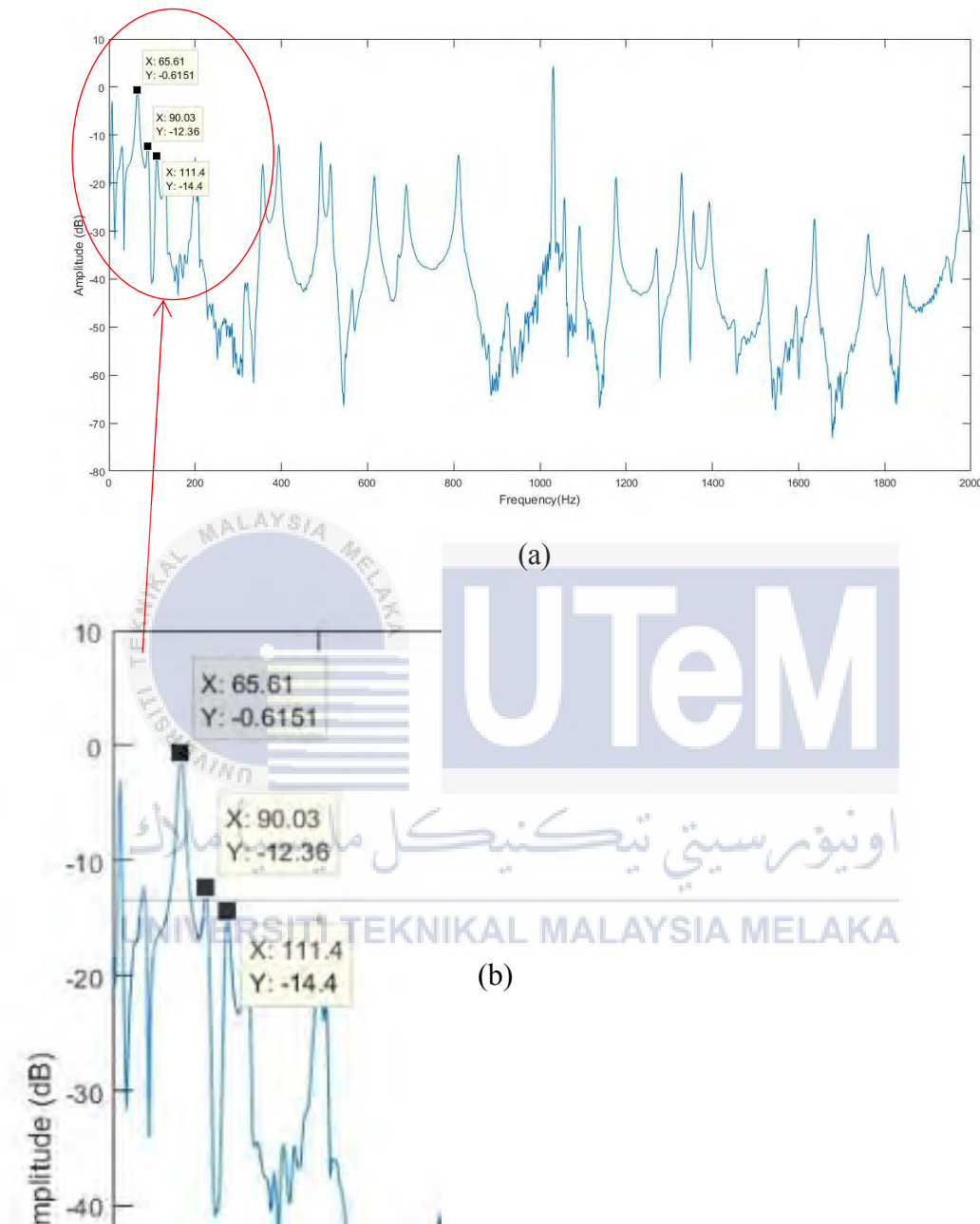


Figure 4-2: FFT result from Matlab (a) original scale (b) magnified scale

Based on the graph of frequency response function, the first three peaks is selected to represent the first 3 frequency mode. The present of high amplitude on the selected frequency might due to the excitation frequency is it corresponding natural frequency. For



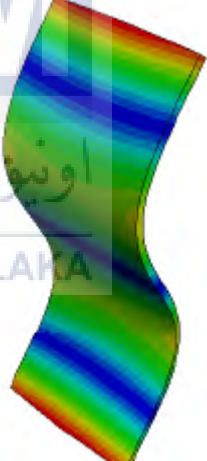
this project, the focus is only on the first three vibration mode. Thus, the three frequencies were excited individually and the respective mode shape was determined using the VL scanning software. The obtained frequencies mode is tabulated as shown in Table 4-2.

Table 4-2: Vibration mode with respective frequency

Vibration mode	1	2	3
Frequency (Hz)	65.61	90.03	111.4

The frequency of 65.61 Hz is the mode 1 which is the first bending mode, 90.03 Hz represented mode 2 which is the first torsion mode and 111.4 Hz the mode 3 represented second bending mode. The mode shape is illustrated as in Table 4-3.

Table 4-3: Vibration mode with respective mode shape

		
Mode 1 65.61 Hz	Mode 2 90.03 Hz	Mode 3 111.4 Hz

4.3 Vibro Acoustic Test

The analysis of average R-value was divided into 3 parts which is 1st sideband analysis, 2nd sideband analysis and 1st + 2nd sideband analysis as in Table 4-4, Table 4-5 and Table 4-6 respectively.

1st sideband analysis

Table 4-4: Average R value based on the 1st sideband

Vibration mode	1	2	3
Frequency (Hz)	65.61	90.09	111.4
Zone	Average R-value		
1	0.326578	0.384306	0.447191
2	0.334367	0.593912	0.517555
3	0.275662	0.359278	0.400877
4	0.085965	0.289761	0.287586
5	0.188135	0.573470	0.504405

UNIVERSITI TEKNIKAL MALAYSIA MELAKA

2nd sideband analysis

Table 4-5: Average R value based on the 2nd sideband

Vibration mode	1	2	3
Frequency (Hz)	65.61	90.09	111.4
Zone	Average R-value		
1	1.821082	1.21761	1.697414
2	1.692859	1.518404	1.536300
3	1.708213	1.461384	1.562484
4	1.547374	1.742600	1.604657
5	1.811911	1.333119	1.449570

1st + 2nd sideband analysis

Table 4-6: Average R value based on the 1st + 2nd sideband

Vibration mode	1	2	3
Frequency (Hz)	65.61	90.09	111.4
Zone	Average R-Value		
1	2.147660	1.601916	2.144605
2	2.027227	2.112317	2.053855
3	1.983875	1.820662	1.963361
4	1.633339	2.032361	1.892243
5	2.000046	1.906589	1.953976

Based on the R-value obtained, a graph was plotted of R-value against distance from crack. So basically the distance from crack would have 5 points which refer to the zone. All three frequency mode was plotted in the same graph for 1st sideband, 2nd sideband and 1st + 2nd sideband analysis result as in Figure 4-3, Figure 4-4 and Figure 4-5 respectively.

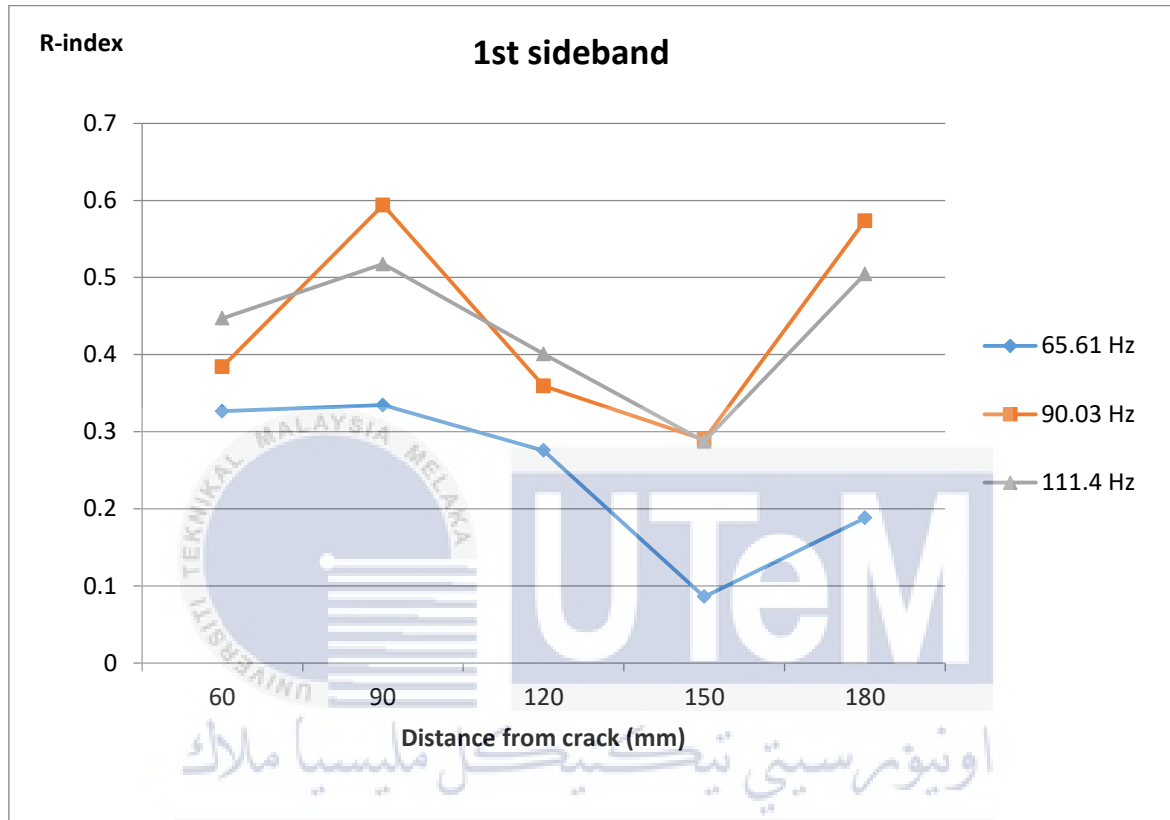


Figure 4-3: Average R-value against distance from crack for 1st sideband analysis

Based on Figure 4-3, all 3 frequency modes shows a similar flow pattern where R-value increases from the distance of 60 mm to 90 mm, decreases from 90 mm to 120 mm, decreases from 120 mm to 150 mm and lastly increases from the 150 mm to 180 mm. The highest R-value presents in mode 2 at zone 2 of 90 mm apart from the crack. Then the lowest R-value is in mode 1 frequency at zone 4 of 120 mm from crack.

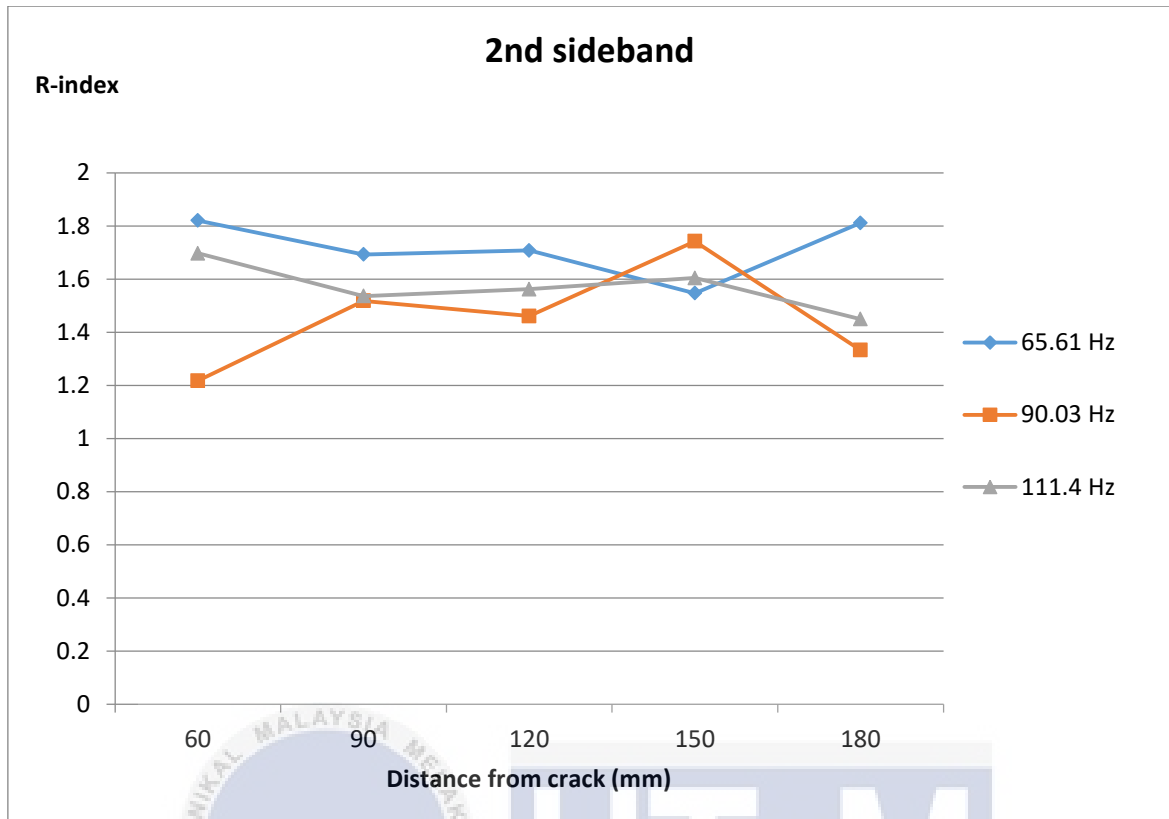


Figure 4-4: Average R-value against distance from crack for 2nd sideband analysis

From Figure 4-4, all the 3 frequency modes show a different type of flow pattern which does not imply any consistency of R-value differing with increase distance from crack. The highest R-value presents in mode 1 at zone 5 which is 180 mm from the crack. In contrast, the lowest value presents in mode 2 at zone 1 which is 60 mm from crack. Then in term of R-value in 2nd sideband, it has a higher average R-value in compare with the R-value from 1st sideband. Averagely the R-value in the 2nd sideband is between 1.2 to 2 rather than 0 to 0.6 in the 1st sideband.

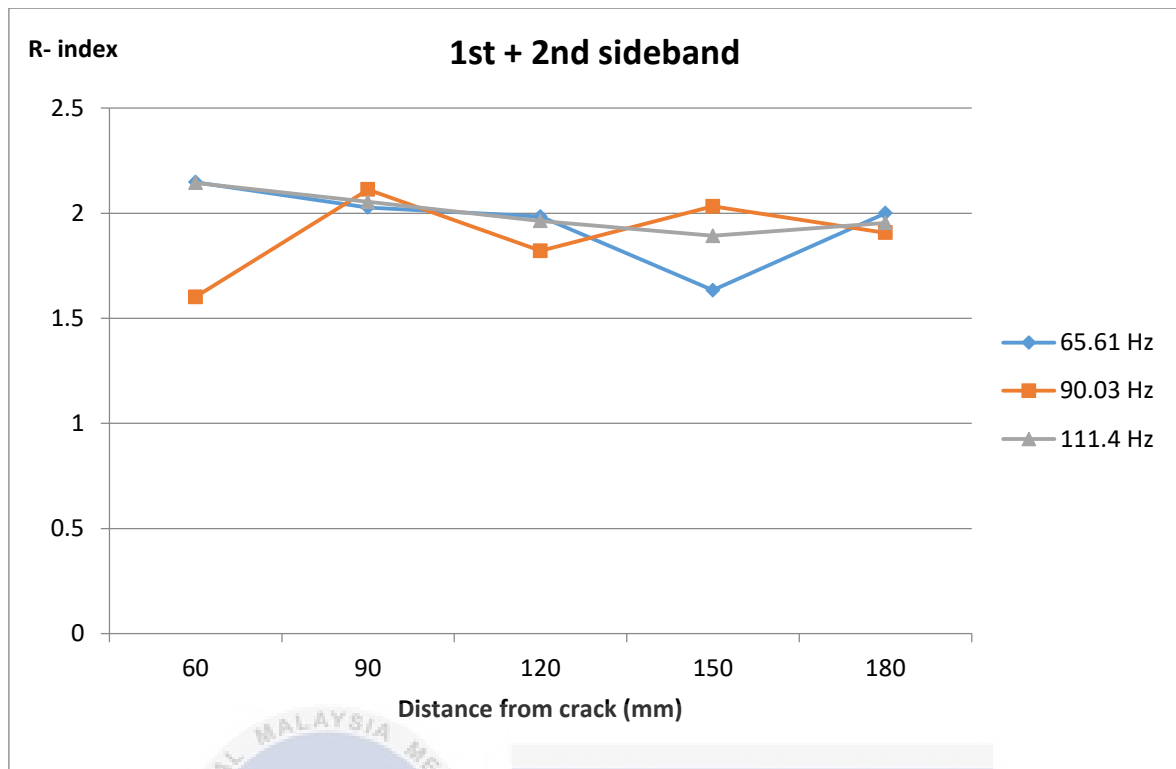


Figure 4-5: Average R-value against distance from crack for 1st + 2nd sideband analysis

Based on Figure 4-5, the mode 1 and mode 3 frequencies has a quite similar flow pattern whereas mode 2 has a repetitive of increasing and decreasing R-value from zone 1 of 60 mm from crack to zone 5 of 180 mm. The highest R-value presents in mode 1 at zone 1 which is 60 mm from the crack. Then the lowest R-value is in mode 2 at zone 1 where it is also 60 mm from crack.

The highest and lowest R-value was tabulated as in Table 4-7.

Table 4-7: Overall result of highest and lowest R-value from the 3 type of sideband analysis

Sideband	Highest R-value	Lowest R-value
1 st	Mode 2, Zone 2 (90 mm)	Mode 1, Zone 4 (150 mm)
2 nd	Mode 1, Zone 5 (180 mm)	Mode 2, Zone 1 (60 mm)
1 st + 2 nd	Mode 1, Zone 1 (60 mm)	Mode 2, Zone 1 (60 mm)

Referring to Table 4-7, it does not display any significant result to justify the relationship between the R-value with the location of measurement point. There is no consistent mode and zone with the highest or lowest R-value. Therefore, contour plot was used to provide a better visualisation for distribution of R-value at all the 25 measurement points for the 3 vibration modes. The distribution is as shown Figure 4-6.

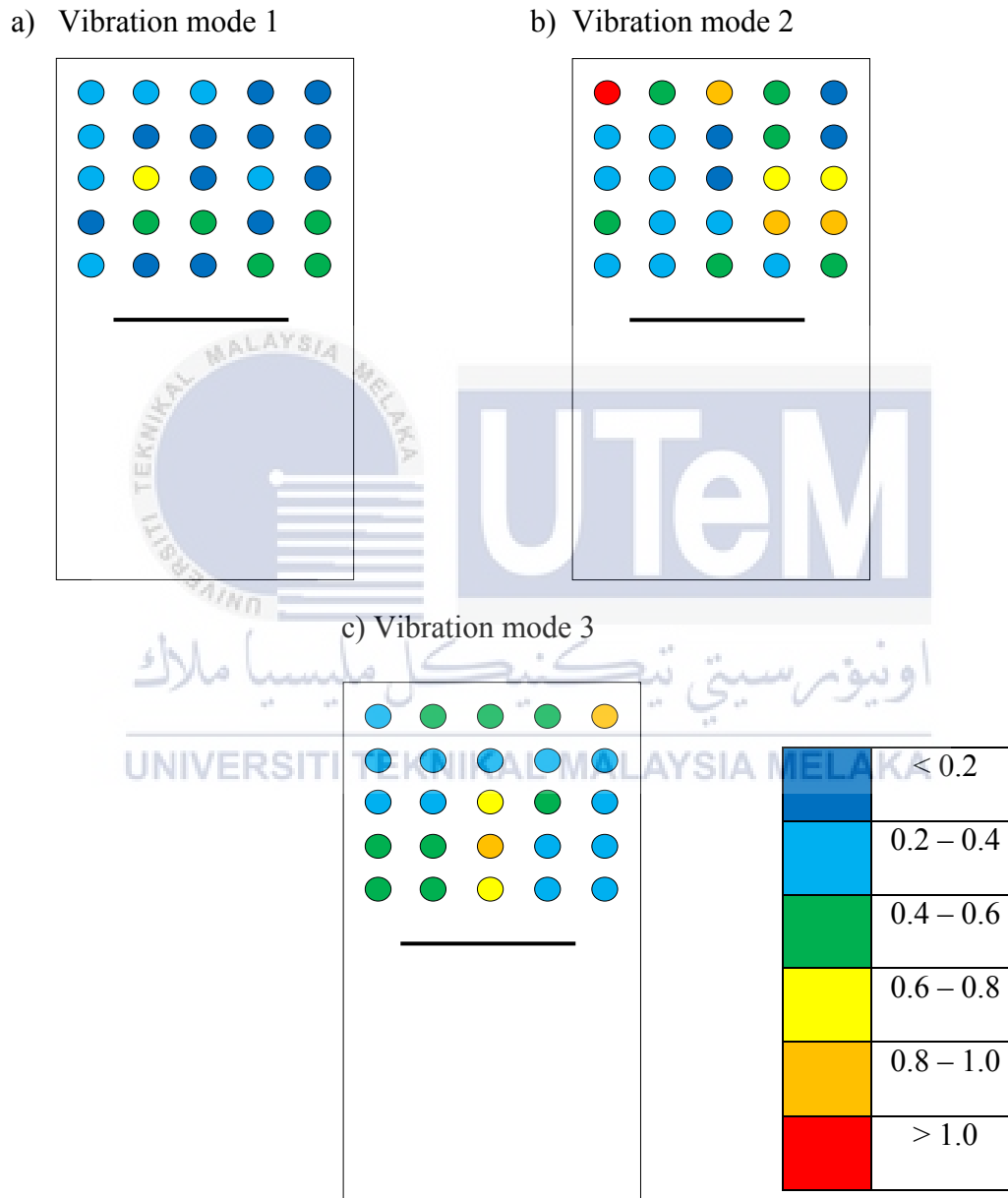


Figure 4-6: Distribution of R-value on the aluminum plate by exciting (a) 1st, (b) 2nd, and (c) 3rd vibration modes.

The distribution of R-value on the aluminum plate resulting from 3 vibration modes does not show any similarity. Based on the contour plot in Figure 4-7, all the 3 vibration modes do not have any consistent pattern with variation of distance from crack. The 1st vibration mode excitation has an average value of 0.22141 which is the lowest among 3 vibration modes. Then is follow by the 3rd vibration mode excitation with value of 0.431523 which is about double the R-value of 1st vibration mode excitation. The highest average R-value is the excitation of 2nd vibration mode with R-value of 0.440146.

4.4 Discussion

The result of location of measurement point effect on modulation intensity (R-value) does not have any similar characteristic. The graph of R-value against distance from crack based on 3 different sideband analysis shows contrasting outcome where all of it displayed a different form of flow pattern graph.

Other than that, the contour plot indication at every point on the aluminum plate has a different modulation intensity level. It could be seen that at higher frequency excitation the average R-value eventually increases, but the modulation intensity at each points towards distance from crack displayed inconsistency.

Thus, it can be concluded that vibro acoustic excitation is valid to detect the crack present in the aluminum plate. This is through the analysis of sidebands present in the spectrum which is the amplitude modulation effect on the wave that passes through crack. However, there is no significant result to justify the correlation between location of measurement points and the modulation intensity.

CHAPTER 5

CONCLUSION & RECOMMENDATION

In conclusion, the vibro acoustic analysis is valid to detect the crack present in the aluminum plate as experiment conducted. There is possibility of higher frequency mode excited would contribute to a higher R-value. Nonetheless, the location of measurement points does not provide any significant indication of the effect on modulation intensity (R-value). Thus, it is very difficult to conclude and verify the correlation between locations of measurement points to the modulation intensity (R-value).

As the result was conducted for only the first 3 mode shapes, in order to verify the conclusion further, an experiment should be conducted for more mode shapes to study the effect of measurement point location on modulation intensity. Other than that, it would display a better analysis of whether a higher frequency mode excitation towards a higher R-value.

REFERENCES

- [1] Ihn, J., Dr. (2016, December 13). Structural Health Monitoring Overview & Aerospace Application. Lecture presented at *Active and sensing materials and their devices*. Retrieved December 15, 2016, from http://courses.washington.edu/mengr568/notes/structural_health_monitoring.pdf.
- [2] Staszewski, W.J., C. Boller, and G.R. Tomlinson, *Health monitoring of aerospace structures: smart sensor technologies and signal processing*. 2004: Chichester: John Wiley & Sons. 266.
- [3] Gdoutos, E.E., *Fracture mechanics: an introduction (Solid mechanics and its applications)*. 2nd ed. Vol. 123. 2005: Norwell, MA Springer Science & Business Media.
- [4] VETTERLEIN, T., GEORGI, S., & TIEDE. (n.d.). *Application of Magnetic Particle Inspection in the Field ...* Retrieved December 15, 2016
- [5] Nelligan, T., & Calderwood, C. (n.d.). *Resources Introduction to Eddy Current Testing*. Retrieved December 15, 2016, from <http://www.olympus-ims.com/en/eddycurrenttesting/>
- [6] Buchler, J., & Berke, M. (n.d.). *Application In Ultrasonic Testing Using Improved Signal Processing Methods*. Retrieved December 15, 2016, from <http://www.ndt.net/article/ecndt02/313/313.htm>
- [7] Raghavan, A., & Cesnik, C. E. (n.d.). Review of *guided-wave structural health monitoring*. Retrieved December 15, 2016, from http://www.academia.edu/2195470/Review_of_guided_wave_structural_health_monitoring
- [8] Staszewski, W.J., C. Boller, and G.R. Tomlinson, *Health monitoring of aerospace structures: smart sensor technologies and signal processing*. 2004: Chichester: John Wiley & Sons. 267.

- [9] Castanedo, C. I., Genest, M., Piau, J. M., Guilbert, S., Bendada, A., & Maldague, X. P. (n.d.). CHAPTER X *ACTIVE INFRARED THERMOGRAPHY TECHNIQUES*. Retrieved December 15, 2016.
- [10] Patricio, M., & Mattheij, R. M. (n.d.). *Crack propagation analysis* - TU/e. Retrieved December 15, 2016, from <https://pure.tue.nl/ws/files/1731130/628883.pdf>
- [11] Bakhary, N., Hao, H., & Deeks, A. J. (2007a). Damage detection using artificial neural network with consideration of uncertainties. *Engineering Structures*, 29(11), 2806-2815.
- [12] Krawinkler, H. (n.d.). *Damage Assessment in steel structures subjected to severe earthquakes*. Retrieved December 15, 2016, from http://www.iitk.ac.in/nicee/wcee/article/8_vol4_887.pdf
- [13] Magi, F., Maio, D. D., & Sever, I. (2016). Damage initiation and structural degradation through resonance vibration: Application to composite laminates in fatigue. *Composites Science and Technology*, 132, 47-56. doi:10.1016/j.compscitech.2016.06.013
- [14] Md Abdul Maleque (3), & Mohd Sapuan Salit (4). (n.d.). *Mechanical Failure of Materials*. Retrieved October 19, 2016, from http://link.springer.com/chapter/10.1007/978-981-4560-38-2_2
- [15] Tee, H. H. (n.d.). Cover feature *Failure Of Structures* - bem.org.my. Retrieved December 15, 2016, from [www.bem.org.my/publication/marchmay04/CF\(Failure\)\(14-20\).pdf](http://www.bem.org.my/publication/marchmay04/CF(Failure)(14-20).pdf)
- [16] Leheta, H. W., Elhewy, A. M., & Younes, H. A. (n.d.). *ANALYSIS OF FATIGUE CRACK GROWTH IN SHIP STRUCTURAL DETAILS*. Retrieved December 15, 2016, from

https://www.researchgate.net/publication/305076816_Analysis_of_Fatigue_Crack_Growth_in_Ship_Structural_Details

[17] Parsons, Z. and W.J. Staszewski, Nonlinear acoustics with low-profile piezoceramic excitation for crack detection in metallic structures. *Smart Materials and Structures*, 2006. 15(4): p. 1110.

[18] Zaitsev, V. and P. Sas, Nonlinear response of a weakly damaged metal sample: A dissipative modulation mechanism of vibro-acoustic interaction. *JVC/Journal of Vibration and Control*, 2000. 6(6): p. 803.

[19] Zaitsev, V.Y., et al., Nonlinear interaction of acoustical waves due to cracks and its possible usage for cracks detection. *JVC/Journal of Vibration and Control*, 1995. 1(3): p. 335.

[20] Nagy, P.B., Fatigue damage assessment by nonlinear ultrasonic materials characterization. *Ultrasonics*, 1998. 36(1-5): p. 375.

[21] Nazarov, V.E., et al., Nonlinear acoustics of micro-inhomogeneous media. *Physics of The Earth and Planetary Interiors*, 1988. 50(1): p. 65.

[22] Morris, W.L., O. Buck, and R.V. Inman, Acoustic Harmonic Generation due to Fatigue Damage in High-Strength Aluminum. *Journal of Applied Physics*, 1979. 50(11 pt 1): p. 6737.

[23] Korotkov, A.S., M.M. Slavinskij, and A.M. Sutin, Variations of acoustic nonlinear parameters with the concentration of defects in steel. *Akusticheskij Zhurnal*, 1994. 40(1): p. 84.

[24] Nagy, P.B., Fatigue damage assessment by nonlinear ultrasonic materials characterization. *Ultrasonics*, 1998. 36(1-5): p. 375.

[25] A. Van Den Abeele, K.E., P.A. Johnson, and A. Sutin, Nonlinear Elastic Wave Spectroscopy (NEWS) Techniques to Discern Material Damage, Part I: Nonlinear Wave

Modulation Spectroscopy (NWMS). Research in *Nondestructive Evaluation*, 2000. 12(1): p. 17.

[26] Donskoy, D.M. and A.M. Sutin, Vibro-acoustic modulation nondestructive evaluation technique. *Journal of Intelligent Material Systems and Structures*, 1999. 9(9): p. 765

[27] Zheng, Y., R.G. Maev, and I.Y. Solodov, Nonlinear acoustic applications for material characterization: A review. *Canadian Journal of Physics*, 1999. 77(12): p. 927.

[28] Hood, A., P. Samuel, and D. Pines. A vibro-acoustic methodology for the detection and characterization of spur gear tooth damage. in *Annual Forum Proceedings - AHS International*. 2005.

[29] Simondi, M., W.J. Staszewski, and R.B. Jenal. Structural damage detection using ultrasonic wave modulation with Low-Profile piezoceramic transducers. in 151 Proceedings of SPIE - *The International Society for Optical Engineering*. 2009. San Diego, CA.

[30] Zaitsev, V.Y., Nazarov, V., Gusev, V. and Castagnede, B., Novel nonlinear-modulation acoustic technique for crack detection. *NDT and E International*, 2006. 39(3): p. 184.

[31] Duffour, P., M. Morbidini, and P. Cawley, A study of the vibro-acoustic modulation technique for the detection of cracks in metals. *Journal of the Acoustical Society of America*, 2006. 119(3): p. 1463.

[32] Meirovitch, L., *Elements of Vibration Analysis*. 1986: MacGraw-Hill, New York

[33] Duffour, P., P. Cawley, and M. Morbidini, Vibro-acoustic modulation NDE technique. Part 1: *Theoretical study*. *Review of Quantitative Nondestructive Evaluation*, 2005. 24: p. 608.

[34] Jenal, R. B. (2010). Fatigue crack detection using nonlinear acoustic: *Analysis of vibro-acoustic modulations*.

[35] Duffour, P., M. Morbidini, and P. Cawley, A study of the vibro-acoustic modulation technique for the detection of cracks in metals. *Journal of the Acoustical Society of America*, 2006. 119(3): p. 1463.

- [36] Duffour, P., M. Morbidini, and P. Cawley, Comparison between a type of vibro-acoustic modulation and damping measurement as NDT techniques. *NDT & E International*, 2006. 39(2): p. 123.
- [37] Van Den Abeele, K.E.A., P.A. Johnson and A. Sutin, Nonlinear Elastic Wave Spectroscopy (NEWS) techniques to discern material damage, Part I: nonlinear wave modulation spectroscopy (NWMS). *Research in Nondestructive Evaluation*, 2000. 12(1): p. 17.
- [38] Polimeno, U. and M. Meo, Detecting barely visible impact damage detection on aircraft composites structures. *Composite Structures*, 2009. 91(4): p. 398. 149
- [39] Zeng, Y., Maev, R. Gr., Solodov I. Y., 'Nonlinear acoustic applications for material characterization: A review) ', *Can. J. Phys*, Vol 77, pp. 927-967, 1999.
- [40] Abeele, V. D., Johnson, P. A., Sutin, A. M., 'Nonlinear elastic wave spectroscopy (NEWS) techniques to discern material damage. part I: Nonlinear wave modulation spectroscopy', *Res Nondestr Eval*, Vol 12, pp. 17-30, 2000.
- [41] Shapiro, R. S., Wagreich, J., Parsons, R. B., Stancato-Pasik, A., Yeh, H. C. & Lao, R., 'Tissue harmonic imaging sonography: Evaluation of image quality compared with conventional sonography', *American Journal of Roentgenology*, Vol 171(5), pp. 1203-1206, 1998.
- [42] Bouakaz, A., De Jong, N., 'Native tissue imaging at superharmonic frequencies', *IEEE Transactions on Ultrasonics, Ferroelectrics, and Frequency Control*, Vol 50(5), pp. 496-506, 2003.
- [43] Khalid C., Leo S, 'Generation of Harmonics at a Real Fatigue Crack Interface', *11th European Conference on Non-Destructive Testing (ECNDT 2014)*, October 6-10, 2014, Prague, Czech Republic
- [44] Hikata, A., Chick, B., and Elbaum, C. *Appl. Phys. Letters* 3 195 (1963)
- [45] Hikata, A. , and Elbaum, C., *Phys. Rev.* 144 469 (1966)
- [46] Buck, O., Morris, W. L., and Richardson, J. M., *Appl. Phys. Letters* 33 371 (1978)
- [47] Broda, D., Pieczonka, L., Hiwarkar, V., Staszewski, W., & Silberschmidt, V. (2016). Generation of higher harmonics in longitudinal vibration of beams with breathing cracks. *Journal of Sound and Vibration*, 381, 206-219.
- [48] Solodov, I.Y., Ultrasonics of non-linear contacts: Propagation, reflection and NDE-applications. *Ultrasonics*, 1998. 36(1-5): p. 383.

- [49] Donskoy, D., A.M. Sutin, and A. Ekimov, Nonlinear acoustic interaction on contact interfaces and its use for nondestructive testing. *NDT and E International*, 2001. 34(4): p. 231.
- [50] Johnson, P.A., The new wave in acoustic testing. *Materials World (UK)*, 1999. 7(9): p. 544-546.
- [51] Sutin, A.M. and P.A. Johnson. Nonlinear elastic wave NDE II. Nonlinear wave modulation spectroscopy and nonlinear time reversed acoustics. in *AIP Conference Proceedings*. 2005. Golden, CO.
- [52] Wu, H.C. and P.F. Pai. Damage detection in concrete and cementitious composites. in *Proceedings of SPIE - The International Society for Optical Engineering*. 2008
- [53] Tournat, V., Zaitsev, V. Yu, Nazarov, V. E., Gusev, V. E. and Castagnede, B., Experimental study of nonlinear acoustic effects in a granular medium. *Acoustical Physics*, 2005. 51(5): p. 543.
- [54] Rantala, J., D. Wu, and G. Busse, Amplitude-modulated lock-in vibrothermography for NDE of polymers and composites. *Research in Nondestructive Evaluation*, 1995. 7(4): p. 215
- [55] Morbidini, M., P. Duffour, and P. Cawley, Vibro-acoustic modulation NDE technique. Part 2: Experimental study. *Review of Quantitative Nondestructive Evaluation*, 2005. 24: p. 616.
- [56] Biemans, C., Staszewski, W. J., Boller, C. and Tomlinson, G. R., Crack detection in metallic structures using broadband excitation of acousto-ultrasonics. *Journal of Intelligent Material Systems and Structures*, 2001. 12(8): p. 589.
- [57] Wu, H.C. Active wave modulation for bond evaluation. in *American Society of Mechanical Engineers (Publication) NDE*. 2002